**COR758, a Negative Allosteric Modulator of $GABA_B$ Receptors**

Alessandra Porcu[a,b*], Rafaela Mostallino[a*], Valeria Serra[a], Miriam Melis[a], Valeria Sogos[a], Sarah Beggiato[c,d], Luca Ferraro[c], Fabrizio Manetti[e], Beatrice Gianibbi[e], Bernhard Bettler[b], Federico Corelli[e], Claudia Mugnaini[#e], and M. Paola Castelli[#a,f,g]

[a]Department of Biomedical Sciences, University of Cagliari, 09042-Monserrato, Italy

[b]Department of Biomedicine, University of Basel, Klingelbergstrasse 50-70, CH-4056 Basel, Switzerland

[c]Department of Life Sciences and Biotechnology, Section of Medicinal and Health Products, and LTTA Center, University of Ferrara, Ferrara, Italy.

[d]Department of Medical, Oral and Biotechnological Sciences, University of Chieti-Pescara, 66100 Chieti, Italy.

[e]Department of Biotechnology, Chemistry, and Pharmacy, University of Siena, I-53100, Siena (SI), Italy.

[f]Guy Everett Laboratory, University of Cagliari, 09042-Monserrato, Italy

[g]Center of Excellence "Neurobiology of Addiction", University of Cagliari, 09042-Monserrato, Italy

**Corresponding author**:

M. Paola Castelli, MD, PhD,
Department of Biomedical Sciences
Division of Neuroscience and Clinical Pharmacology,
Cittadella Universitaria, SS 554, km. 4,500,
I-09042 Monserrato (CA), ITALY.
Telephone: +39-070-6754065;
FAX: +39-070-6754320,
e-mail:castelli@unica.it

[#*]These authors contributed equally to the study

**Abbreviations**

**BRET, Bioluminescence resonance energy transfer**

**CAMYEL, cAMP sensor using YFP-EPAC-Rluc**

**CNS, Central nervous system**

**CHO, Chinese Hamster Ovary**

**GDP, Guanosine 5′-diphosphate**

**GTPγS, guanosine 5′-O-(3-thiotriphospate)**

**HEK-293, Human Embryonic Kidney 293**

**Abstract**

Allosteric modulators of G protein coupled receptors (GPCRs), including $GABA_BRs$ ($GABA_BRs$), are promising therapeutic candidates. While several positive allosteric modulators (PAM) of $GABA_BRs$ have been characterized, only recently the first negative allosteric modulator (NAM) has been described. In the present study, we report the characterization of COR758, which acts as $GABA_BR$ NAM in rat cortical membranes and CHO cells stably expressing $GABA_BRs$ (CHO-$GABA_B$). COR758 failed to displace the antagonist [$^3$H]CGP54626 from the orthosteric binding site of $GABA_BRs$ showing that it acts through an allosteric binding site. Docking studies revealed a possible new allosteric binding site for COR758 in the intrahelical pocket of the $GABA_{B1}$ monomer. COR758 inhibited basal and $GABA_BR$-stimulated O-(3-[$^{35}$Sthio)-triphosphate ([$^{35}$S]GTPγS) binding in brain membranes and blocked the enhancement of $GABA_BR$-stimulated [$^{35}$S]GTPγS binding by the PAM GS39783. Bioluminescent resonance energy transfer (BRET) measurements in CHO-$GABA_B$ cells showed that COR758 inhibited G protein activation by GABA and altered $GABA_BR$ subunit rearrangements. Additionally, the compound altered $GABA_BR$-mediated signaling such as baclofen-induced inhibition of cAMP production in transfected HEK293 cells, agonist-induced $Ca^{2+}$ mobilization as well as baclofen and the ago-PAM CGP7930 induced phosphorylation of extracellular signal-regulated kinases (ERK1/2) in CHO-$GABA_B$ cells. COR758 also prevented baclofen-induced outward currents recorded from rat dopamine neurons, substantiating its property as a NAM for $GABA_BRs$. Altogether, these data indicate that COR758 inhibits G protein signaling by $GABA_BRs$, likely by interacting with an allosteric binding-site. Therefore, COR758 might serve as a scaffold to develop additional NAMs for therapeutic intervention.

**Key words**: $GABA_B$ receptors, Allosteric modulators, Negative allosteric modulator (NAM), GTPγS binding, Bioluminescence resonance energy transfer (BRET)

## 1. Introduction

The $GABA_BR$, a G protein coupled receptor (GPCR), mediates metabotropic actions of the major inhibitory neurotransmitter GABA in the central nervous system (CNS). $GABA_BRs$, widely expressed and distributed in the CNS, are functional heterodimers composed by two subunits, $GABA_{B1a/b}$ and $GABA_{B2}$ (Kaupmann et al., 1998). Recently, it has also been demonstrated that potassium channels tetramerization domain-containing (KCTD) proteins tightly associate with $GABA_BRs$ in the brain to influence the kinetics of the receptor response (Schwenk et al., 2010; Turecek et al., 2014; Rajalu et al., 2015; Zheng et al., 2019). $GABA_BRs$ activate several distinct intracellular signal transduction pathways (Guyon and Leresche, 1995; Pin and Bettler, 2016) via Gi/o proteins, inhibit adenylate cyclase, and control $K^+$ (Kir3) and $Ca^{2+}$ channel activity (Kulik et al., 2006; Park et al., 2010; Gassmann and Bettler, 2012). Furthermore, $GABA_BRs$ induce extracellular signal-regulated kinases 1 and 2 (ERK1/2) phosphorylation in the CA1 region of the hippocampus, in cultured cerebellar neurons and–human embryonic kidney cell (HEK293) cells overexpressing $GABA_BRs$ (Sun et al., 2016, Tu et al., 2007). Widespread distribution of $GABA_BRs$ in the brain and their involvement in multiple signaling pathways implicates them in a wide range of psychiatric and neurological disorders (e.g. pain, spasticity, anxiety and depression, absence epilepsy, drug addiction, cognition) (Bettler et al., 2004; Bowery, 2006; Enna and McCarson, 2016; Felice et al., 2016; Frankoswska et al., 2016; Agabio et al., 2016). Accordingly, preclinical and clinical studies have demonstrated efficacy of $GABA_BR$ agonists in several neurologic and psychiatric disorders, including alcohol use disorder (Millan, 2002, 2003; Mombereau et al., 2004, 2005; Gambardella et al., 2003; Roberts et al., 1996; Prosser et al., 2001; Tao and Auerbach, 2002; Froestl, 2010; de Beaurepaire et al., 2019). $GABA_BR$ antagonists might be useful candidates for treating cognitive dysfunctions and depression (Schuler et al., 2001; Froestl et al., 2004; Cryan and Kaupmann, 2005), absence epilepsy and Down's syndrome (Froestl, 2010). $GABA_BRs$ antagonists have antidepressant-like effects in several animal models of depression, *i.e.* learned helplessness, olfactory bulbectomy and chronic mild stress (Frankowska et al., 2007; Nakagawa et al., 1999; Nowak et al., 2006; Slattery

et al., 2005; Jacobson et al., 2018). Placebo-controlled phase 2 clinical trials in patients treated with the orally active $GABA_BR$ antagonist CGP36742 showed significant improvement in working memory, psychomotor speed, and attention compared with placebo (Froestl et al., 2004). To date, however, baclofen (Lioresal®) is the only marketed $GABA_BR$ agonist, used in the treatment of spasticity and spinal cord injuries. In October 2018, baclofen has also been officially approved in France for treating alcohol use disorders (AUD) https://www.ansm.sante.fr/S-informer/Communiques-Communiques-Points-presse/L-ANSM-octroie-une-autorisation-de-mise-sur-le-marche-pour-une-utilisation-du-baclofene-dans-l-alcoolo-dependance-Communique).

Besides the well-known effects of $GABA_BR$ agonists and antagonists, the recent discovery of allosteric modulators for $GABA_BRs$ has provided new tools for their pharmacological manipulation. While competitive ligands bind to the orthosteric binding site within the Venus flytrap domain (VFD) of the $GABA_{B1a/b}$ subunit, the $GABA_BR$ positive allosteric modulators (PAMs) GS39783 and CGP7930 act through the heptahelical domain (HD) of the $GABA_{B2}$ subunit (Binet et al., 2004; Dupuis et al., 2006). PAMs, being almost devoid of intrinsic agonist activity *per se*, increase both potency and efficacy of GABA and orthosteric $GABA_BR$ agonists (see Urwyler, 2011). Several other $GABA_BR$ PAMs, such as BHFF, NVP-BHF177, ADX71441, COR627, COR628, COR659 and SSD114, have been identified (Urwyler et al., 2001, 2003; Malherbe et al., 2008; Castelli et al., 2012, Mugnaini et al., 2013; Porcu et al., 2016; Mugnaini and Corelli, 2016). Although PAMs were found to have no, or weak agonist-allosteric modulator activity (ago-PAM) when applied alone, some of the $GABA_BR$ PAMs (e.g., CGP7930) exhibits assay-dependent ago-PAM activity (Binet et al., 2004; Tu et al., 2007; Chen et al., 2014).

In vivo, $GABA_BR$ PAMs potentiated the sedative/hypnotic effect of baclofen (Carai et al., 2004; Koek et al., 2010), and showed efficacy in animal models of anxiety (Cryan et al., 2004; Jacobson and Cryan, 2008; Li et al., 2013) and alcohol and nicotine abuse (Paterson et al., 2008; Maccioni et al., 2009; Agabio and Colombo, 2014). Importantly, because of their mechanism of action (i.e., modest or no intrinsic agonist activity), $GABA_BR$ PAMs are expected to have less side effects and a

higher therapeutic index than agonists (Kalinichev et al., 2014; Pin and Prezeau, 2007; Urwyler, 2016). Although the blockade of $GABA_BRs$ by negative allosteric modulators (NAMs) might represent a relevant therapeutic tool for several CNS diseases, the first NAM has only been described recently (Chen et al., 2014). The authors found that CLH304a negatively modulated $GABA_BR$ activity through the HD of the $GABA_{B2}$ subunit (Chen et al., 2014; Sun et al., 2016). Thus, such results offer opportunities for therapeutic intervention based on $GABA_BR$ inhibition through allosteric modulation.

In the present study, we focused on the characterization of 4-hydroxy-1-isobutyl-3, 6-diisopropylquinolin-2(1*H*)-one (COR758) described by Mugnaini et al. (2020), where it is referred to as compound 17f. COR758 was designed as an analogue of rac-BHFF, with the aim of identifying new $GABA_BR$ PAMs characterized by improved chemical accessibility and potential for drug development. On this basis, the benzofurane scaffold of rac-BHFF was replaced with an achiral and planar 2-quinolone system, retaining to some extent the substitution pattern of the parent molecule. Unexpectedly, functional assays revealed that COR758 switched to a NAM/antagonist.

Here, we report that COR758 fails to displace the antagonist [$^3$H]CGP54626 from the orthosteric binding site of $GABA_BRs$ and inhibits GABA-stimulated O-(3-[$^{35}$Sthio)-triphosphate ([$^{35}$S]GTPγS) binding using a native $GABA_BR$ preparation (rat cortical membranes), thus confirming and extending our previous findings (Mugnaini et al., 2020). Docking analysis revealed putative binding sites of COR758 in a new intrahelical binding pocket of the $GABA_{B1}$ monomer. Bioluminescent resonance energy transfer (BRET) measurements in living CHO cells stably expressing $GABA_BRs$ (CHO-$GABA_B$) show that COR758 prevents receptor activation by GABA and dissociation of the heterotrimeric G protein. Additionally, as shown in BRET experiments, COR758 influences the conformation of the heterodimeric assembly of $GABA_BRs$ and prevents GABA-mediated inhibition of adenylate cyclase activity. COR758 also inhibits baclofen- and the ago-PAM CGP7930-induced ERK1/2 phosphorylation in CHO-$GABA_B$ cells as well as baclofen-induced increases in intracellular $Ca^{2+}$ levels in HEK293 co-expressing $GABA_{B1a}$ and $GABA_{B2}$ together with a chimeric Gα protein.

In addition, COR758 abolishes baclofen-induced outward currents in dopamine neurons in acute slices of the ventral tegmental area (VTA). Overall, our data indicate that COR758 acts as a NAM and negatively modulates $GABA_BR$ function/activity.

## 2. Material and Methods

### *2.1 Animals*

All procedures and experiments were carried out according to Italian (D.L. 26/2014) and European Council Directive (63/2010) and in compliance with the approved animal policies by the Ethical Committee for Animal Experiments (CESA, University of Cagliari) and the Italian Department of Health. All possible efforts were made to minimize animal pain and discomfort and to reduce the number of experimental subjects. Male Sprague Dawley rats (Envigo, Italy), weighing 200 to 250 g were used; for electrophysiological experiments the rats were used at 16-22 postnatal day. They were housed 4 per cage in standard plastic cages with-fir chips bedding-in standard conditions (20-21°C, 60% humidity and a 12-h light cycle) food and water being available ad libitum.

### *2.2 Drugs and plasmid constructs*

GABA, GDP, and GTPγS, were obtained from Sigma/RBI (Natick, MA, USA); CGP54626 and (R)-Baclofen were from Tocris Bioscience (Ellisville, MO, USA). [$^{35}$S]GTPγS (125 Ci/mM) and [$^{3}$H]CGP54626 (85 Ci/mM) were obtained from PerkinElmer and from American Radiolabeled Chemicals Inc. (St. Louis, MO, USA), respectively. Drugs were dissolved in 100% DMSO and then diluted in an assay buffer. The concentration of DMSO used in the different assays never exceeded 0.1% (v/v) and had no effects on [$^{3}$H]CGP54626 and [$^{35}$S]GTPγS binding assay, electrophysiological recordings, western and BRET measurements. Luciferase substrate, Coelenterazine, was purchased from NanoLight Technologies (US), Lipofectamine 2000 transfection reagents were obtained from Thermo Fisher Scientific (Waltham, MA). The plasmid pcDNA3L-His-(cAMP sensor using YFP-Epac-RLuc) (CAMYEL, MBA-277) (Jiang et al., 2007) was purchased from ATCC. $G\alpha_o$-Rluc, $G\gamma_2$-

Venus, Gβ1-Flag, Gγ2-HA were a kind gift from Jean Philippe Pin (Institute of Functional Genomics, Montpellier, France), $GABA_{B1a}$-RLuc and -$GABA_{B2\text{-}YFP}$ were obtained by adding a RLuc-tag and GFP-tag at the C-terminal end of $GABA_{B1a}$ and $GABA_{B2}$, respectively.

*2.3 Synthesis and molecular modelling studies of 4-hydroxy-1-isobutyl-3,6-diisopropylquinolin-2(1H)-one (COR758)*

*2.3.1.* The target molecule was obtained according to the procedure reported by Mugnaini et al., 2020.

*2.3.2.* The cryo-EM structure of the full-length $GABA_B$ receptor in an inactive conformation (entry 7c7s of the protein data bank) (Mao, 2020) was chosen to perform molecular docking simulations. The Protein Preparation wizard of the Schrodinger suite (Maestro, release 2019-2. Schrödinger, LLC, New York, NY, 2019) was used to add hydrogen atoms and optimize their positions. The structure of COR758 was sketched with Maestro and submitted to the LigPrep routine that generated possible ionization and tautomeric states. SiteMap (Halgren, 2009) was then used to identify potential binding sites on the overall receptor structure. The physicochemical properties of each potential binding site were codified to be used for molecular docking simulations. Glide software was used for standard-precision docking, taking ligand flexibility into account during calculations. Ligand binding poses were ranked based on default scoring functions.

*2.4 Binding studies*

*2.4.1. Membrane preparation for binding assays*

Membrane preparation was carried out as previously described (Castelli et al., 2012). Briefly, rats (250 g) were sacrificed, their brains rapidly removed and cerebral cortices were dissected on ice. Cortical tissues were homogenized using a glass-teflon homogenizer (Glass-Col, Terre Haute, IN, USA) in 15 volumes (v/w) of ice-cold 0.32 M sucrose and 1mM EDTA. The homogenate was

centrifuged at 1000 g for 10 min, and the supernatant was collected and recentrifuged at 20,000 x g for 20 min. The pellet was re-suspended in 20 volumes (v/w) of ice-cold distilled water, homogenized using a Polytron homogenizer, and centrifuged at 8000 x g for 20 min. The last centrifugation of supernatant together with the buffy layer was performed at 45,000 x g for 40 min; the supernatant was discarded, and the final pellet was frozen and stored at -80°C for at least 24 h before use both for [$^{3}$H]CGP54626 binding assay and [$^{35}$S]GTPγS binding assay for $GABA_BR$. The Bradford (1976) protein assay was used for protein determination using bovine serum albumin as a standard according to the supplier's protocol (Bio-Rad, Milan, Italy).

*2.4.2 [$^{3}$H]CGP54626 binding assay.*

Membrane pellets were thawed at 4 °C and prepared as previously described (Castelli et al., 2012; Porcu et al., 2016). [$^{3}$H]CGP54626 binding was performed using 50 µg of membrane proteins and 2 nM [$^{3}$H]CGP54626 in a final volume of 1 ml of Krebs Henseleit buffer (NaCl 143 mM, Tris 50 mM, KCl 5.9 mM, $MgSO_4$ 1.2 mM, $CaCl_2$ 2.5 mM, pH 7.4) at 22–24°C for 30 min. Nonspecific binding was estimated in the presence of 10 µM unlabeled CGP54626. Free ligand was separated from bound ligand by rapid filtration through Whatmann GF/B glass filters using a Brandel 30-sample harvester (Brandel Inc., Gaithersburg, MD). Filters were then rinsed twice with ice-cold Krebs-Henseleit buffer. Filter-bound radioactivity was counted using 3 ml of scintillation fluid (Ultima Gold MV; PerkinElmer Life and Analytical Sciences) in a liquid scintillation counter (Tri-Carb 2810; PerkinElmer Life and Analytical Sciences). [$^{3}$H]CGP54626 displacement curves were performed using serial dilutions ranging from $10^{-10}$ to $10^{-7}$ or $10^{-10}$ to $10^{-4}$ of CGP54626 or COR758, respectively. The calculation of $IC_{50}$ was performed by non-linear curve fitting of the concentration-effect curves using the Graph Pad Prism Program (San Diego, CA, USA). The F-test was used to determine the best approximation of a non-linear curve fitting to one or two site model ($p< 0.05$).

*2.4.3. [$^{35}$S]GTPγS binding assay*

On the day of the experiment, the frozen rat cortex membranes were thawed at 4°C, prepared as previously described (Castelli et al., 2012). Subsequently membrane homogenates and drugs were

preincubated in PerkinElmer PicoPlates 96 (300 µl volume) for 30 min at 30°C. The main incubation was then started by the addition of [$^{35}$S]GTPγS to a final concentration of 0.2 nM. After a 40-min incubation at 30°C, the samples were filtered using a PerkinElmer UniFilter-GF/B, washed twice with 300 µl of buffer, and dried for 1 h at 30°C. The radioactivity on the filters was counted in a liquid microplate scintillation counter (TopCount NXT; PerkinElmer Life and Analytical Sciences). Basal binding was assessed in the absence of agonist and in the presence of GDP, and nonspecific binding was measured in the presence of 10 µM unlabeled GTPγS. The stimulation by agonist was defined as the percentage increase above basal levels (i.e., [disintegrations per minute (agonist) - disintegrations per minute (no agonist)/(disintegrations per minute (no agonist)] × 100). Data are reported as the mean SEM of three to six experiments, performed in triplicate.

*2.5. Cell cultures and BRET measurements.*

Culture and maintenance of CHO-K1 cells stably expressing human $GABA_{B(1b)}$ and rat $GABA_{B2}$ (CHO-$GABA_B$) were performed as described previously (Urwyler et al., 2001). For G-protein activity measurement CHO-$GABA_B$ were transfected with $G\alpha_o$-Rluc, $G\gamma_2$-Venus, $G_{\beta1}$-Flag. For cAMP responses measurement CHO-$GABA_B$ were transiently co-transfected with pcDNA3L-His-CAMYEL. 24 h after transfection, cells were washed twice with PBS and incubated in the presence or absence of COR758 (different concentrations) for 15 min before substrate addition in a 96-well microplate. BRET measurement was initiated using the Infinite® F500 microplate reader (Tecan, Switzerland) after 10 min of incubation with 5 µM Coelenterazine h (NanoLight Technologies, Pinetop, AZ, USA). Luminescence and fluorescence signals were detected sequentially with an integration time of 200 ms. The BRET ratio was calculated as the emission of YFP (530–570 nm) over the emission of RLuc (370–470 nm). The curves were fitted using Graph Pad Prism 5.0 ("Plateau followed by one-phase decay" for G-protein activity and "Plateau followed by one-phase association" for CAMYEL activity). The amplitude-weighted mean time constant (tau) was obtained by fitting the

BRET recovery phase to a double exponential function. ΔBRET was calculated as the difference between the basal and the plateau of the BRET signal.

For $GABA_BR$ conformational changes measurements, CHO-K1 cells were transfected with $GABA_{B1a}$-Rluc and $GABA_{B2}$-YFP. 24 h after transfection the cells were washed twice with PBS and incubated with COR758 as described above. The BRET ratio was calculated as the ratio of light emitted by YFP (530–570 nm) over the light emitted by RLuc (370–470 nm). The curves were fitted using GraphPad Prism 5.0 ("Plateau followed by one-phase decay"). The amplitude-weighted mean time constant (tau) was obtained by fitting the BRET recovery phase to a double exponential function. ΔBRET was calculated as the difference between the basal and the plateau of BRET signal.

*2.6 Intracellular calcium measurement in CHO-$GABA_B$ cell*

Stable cell lines expressing the human $GABA_B$ ($hGABA_B$) receptor coupled with a chimeric Gα protein allowing redirection of the activation signal to intracellular calcium flux were used to characterize the pharmacological activity of COR758 at $hGABA_BR$. To this purpose, the method previously described by Kalinichev et al. (2014) has been used. Twenty-four hours before the experiment, $hGABA_BR$-transfected HEK293 cells were plated out at a density of 30,000 cells per well in black, clear bottom plates (Corning®; Sigma-Aldrich, Milan, Italy) in glutamine/glutamate-free DMEM containing 10% decomplemented FBS, 100 U/mL penicillin and 100 µg/mL streptomycin, supplemented with 1 µg/mL doxycycline. Cells were incubated at 37°C with 5% $CO_2$ in a humidified atmosphere. After 24 h of incubation, cells were loaded with Hank's Balanced Salt Solution (HBSS) supplemented with 2.5 mM probenecid (Merck Life Science, Milan, Italy), 3 µM of the calcium sensitive fluorescent dye Fluo-4 AM (Thermo-Fisher Scientific, Waltham, MA, United States), 0.01% pluronic acid and 20 mM HEPES (pH 7.4; Merck Life Science, Milan, Italy) for 30 min at 37°C. Afterwards the loading solution was aspirated, a washing step with 100 µl/well of HBSS, HEPES (20 mM, pH 7.4), 2.5 mM probenecid and 500 µM Brilliant Black (Merck Life Science, Milan, Italy) was carried out. Subsequently 100 µl/well of the same buffer were added for 10 min.

Concentrated solutions of ligands (*i.e.*, GABA, baclofen and COR 758) were freshly prepared and serial dilutions were made in HBSS/HEPES (20 mM) buffer (containing 0.02% BSA fraction V). After placing cell culture and compound plates into the FlexStation II (Molecular Devices, Sunnyvale, CA, United States), the on-line additions were carried out in a volume of 50 µl /well and fluorescence changes were continuously measured for 2 min at 37°C. The calcium peak level has been then selected to evaluate the effects of treatments (Beggiato et al., 2018).

$EC_{50}$ values were calculated using non-linear regression [curve fit, log(agonist) vs. response, variable slope, four parameters]. Statistical analysis (F-test) has been performed by using GraphPad Prism 6.0 (GraphPad Software Inc., San Diego, CA, United States). Statistical differences between group means for $EC_{50}$ values were also assessed by ANOVA followed by Tukey's multiple comparisons test. Data are reported as mean ± SEM of three independent experiments. A p-value < 0.05 was considered statistically significant (Beggiato et al., 2018).

*2.7 Glutamate efflux measurement on synaptosomes*

*2.7.1 Synaptosome preparation*

Crude synaptosome (P2) fraction was prepared from male Sprague-Dawley rat brain (Ferraro et al., 2010). Briefly, the animal was sacrificed under light anesthesia, the brain removed and the frontal cortex or the striatum was rapidly dissected out. The tissue was then homogenized in ice-cold buffered sucrose solution (0.32 M, pH-7.4). The homogenate was centrifuged (10 min; 2500 × g, 4°C) and synaptosomes isolated from the supernatant by centrifugation (20 min; 9500 × g, 4°C). The P2 pellet was resuspended in 7 ml of Krebs solution (mM: NaCl 118.5, KCl 4.7, $CaCl_2$ 1.2, $KH_2PO_4$ 1.2, $MgSO_4$ 1.2, $NaHCO_3$ 25, glucose 10; gassed with 95% $O_2$/5% $CO_2$).

*2.7.2 Spontaneous endogenous glutamate efflux*

Identical aliquots of synaptosomal suspension were distributed on microporous filters (0.5 ml/filter) and placed at the bottom of a set of parallel superfusion chambers maintained at 37°C. Synaptosomes were perfused with aerated (95% $O_2$/5% $CO_2$) Krebs solution (flow = 0.3 ml/min). After 30 min, 5-

min fractions were collected from the 30$^{th}$ to the 75$^{th}$ min (9 samples). When required, baclofen (10 μM), quinpirole (1 μM) or COR 758 (1-30 μM) were added, either alone or in combination, to the perfusion medium from the fourth sample till the end of the experiment. Control synaptosomes perfused with Krebs' solution were assayed in parallel.

*2.7.3 $K^+$-evoked glutamate efflux*

After the collection of three basal samples, synaptosomes were depolarized with 15 mM $K^+$ (substituting for an equimolar concentration of NaCl) for 90 s. When required, baclofen (10 μM), quinpirole (1 μM) or COR 758 (1-30 μM) were added, either alone or in combination, to the perfusion medium concomitantly with the depolarizing stimulus.

*2.7.4 Endogenous glutamate assay*

Thirty microliter aliquots were used to quantify endogenous glutamate levels by a HPLC/fluorimetric detection system, including precolumn derivatization with o-phthaldialdehyde reagent and Chromsep 5 (C18) column (mobile phase: 0.1 M sodium acetate, 10% methanol, 2.5% tetrahydrofurane, pH 6.5) (Ferraro et al., 1995). No drugs under investigation interfered with the glutamate assay.

$K^+$-evoked glutamate efflux was expressed as percent increase over the spontaneous release (mean of the two fractions collected prior to the depolarizing stimulus). The effect of treatment was expressed as percentage ratio of the depolarization-evoked neurotransmitter overflow calculated in the presence of the drug versus that obtained under control conditions, always assayed in parallel.

Statistical analysis was carried out by Student's t test or one-way analysis of variance (ANOVA) followed by the Newman-Keuls test for multiple comparisons.

*2.8 ERK1/2 phosphorylation detection in CHO-$GABA_B$ and CHO-D2 cell.*

ERK1/2 phosphorylation induced by the $GABA_BR$ agonist and D2 dopamine receptor agonist was measured in CHO-$GABA_B$ and in CHO-K1 cells stably expressing human D2 dopamine long receptor (CHO-D2), respectively. Culture and maintenance of CHO-D2 were performed as previously described (Porcu et al., 2018). CHO-$GABA_B$ cell cultures were washed with Hank's Balanced Salt

Solution (HBSS) (Ca2+ free) and then incubated with HBSS at 37°C for 60 min. Cells were treated for 2.5 min with the agonist $GABA_BR$ baclofen (100 µM) or the PAM $GABA_BR$ CGP7930 (100 µM). For antagonist and NAM treatment cells were pretreated for 20 min before agonist or PAM treatment with 100 µM of the $GABA_BR$ antagonist GCP54626 or 100 µM of the compound COR758. CHO-D2 cells were grown to 80% confluence, rinsed with serum free Minimum Essential Medium Eagle (MEM) and incubate overnight in serum-free MEM. Cell were incubated with dopamine (1 µM) or the D2 dopamine receptor agonist quinpirole (1 µM) for various times. In antagonist experiments, cells were preincubated for 5 min with the D2 dopamine receptor antagonist haloperidol (1 µM) or the compound COR758 (100 µM). At the end of treatment CHO-$GABA_B$ or CHO-D2 cells were quickly washed with ice-cold PBS pH 7.4, resuspended in 200 µl of SDS 2%, processed for western blot analysis and stored at – 80° C until use. Protein concentrations were determined using Pierce BCA Protein assay (Waltham, Massachusetts, USA) (using bovine serum albumin as a standard) following the company's protocol. Samples with equal amounts of protein (20 µg) mixed with Laemmli loading buffer were denatured at 100°C for 3 min and loaded on 12% sodium dodecyl sulfate (SDS)-polyacrylamide gel electrophoresis (SDS-PAGE). In parallel to the samples, internal molecular weight (MW) standards (Precision Plus Protein Western C Standards, Bio-Rad, Hercules, CA, USA) were run to identify the specific bands. Proteins were transferred to polyvinylidene difluoride (PVDF) membranes following the company's protocol (Amersham GE Healthcare, UK). Membranes were blocked for 1 hour at room temperature (RT) using a mixture of 20 mM Tris base, 137 mM sodium chloride and 0.1% Tween 20 (TBS-T) containing 5% milk powder, before incubation overnight at 4 °C with the primary antibodies. The following antibodies were used: rabbit polyclonal antibodies against pospho-ERK1/2 (1:1000) and total ERK1/2 (1:1000) (Cell signaling Technology, Beverly, MA, USA); mouse antibody against Glyceraldehyde-3-phosphate dehydrogenase (GADPH) (1:1000) (MAB374 Millipore, Merck MA, USA). Blots, were incubated at RT for 1 h with goat IgG anti-rabbit horseradish peroxidase (HRP) conjugated (1:10,000: Millipore) or goat IgG anti-mouse HRP conjugated ( 1:5000; Vector, CA, USA) and after TBS-T rinse, protein bands were developed

using the Clarity Western ECL Substrate, (Bio-Rad, Hercules, California) according to the protocol provided by the company, and visualized by ImageQuant LAS-4000 (GE Healthcare, Little Chalfont, UK). The signals of the specific bands were normalized with the densities of the corresponding band of GAPDH, used as a loading control. The ratio of the density of total ERK1/2 and pErk1/2 bands to the density of GAPDH ones was used to compare relative expression levels of these proteins in CHO-GABAB and CHO-D2 cells. . Densitometry analysis was performed by Image Studio Lite Software (RRID:SCR_014211, Li-Cor, http://www.licor.com/bio/products/software/image_studio_lite/)

*2.9 Electrophysiology: Whole-cell voltage clamp recordings from dopamine neurons*

Whole-cell patch-clamp recordings from midbrain dopamine cells were as previously described (Melis et al., 2010). Briefly, male Sprague Dawley (PND 14-25) rats were anesthetized with isoflurane and killed. Recordings were made from horizontal hemi-slices (300 μm) superfused with artificial cerebrospinal fluid (ACSF, at 37°C), saturated with 95% $O_2$ and 5% $CO_2$ containing (in mM): 126 NaCl, 1.6 KCl, 1.2 $NaH_2PO_4$, 1.2 $MgCl_2$, 2.4 $CaCl_2$, 18 $NaHCO_3$ and 11 glucose. Voltage-clamp experiments were performed with electrodes filled with a solution containing the following in mM: 144 KCl, 10 HEPES, 3.45 BAPTA, 1 CaCl, 2.5 $Mg_2ATP$, and 0.25 $Mg_2GTP$ (pH 7.2 - 7.4, 275 - 285 mOsm). Dopamine neurons from lateral portion of the posterior VTA (i.e., medial to the medial terminal nucleus of the accessory optic tract) were identified by the presence of a large $I_h$ current (Johnson and North, 1992) that was assayed immediately after break-in using a series of incremental 10 mV hyperpolarizing steps from a holding potential of -70 mV. Cells were visualized using an upright microscope with infrared illumination (Axioskop FS 2 plus, Zeiss), and whole-cell patch-clamp recordings were made using an Axopatch 200B amplifier (Molecular Devices). Data were filtered at 2 kHz, digitized at 10 kHz, and collected on-line with acquisition software (pClamp 10.6, Molecular Devices).

Whole-cell outward $K^+$ currents were recorded in the presence of picrotoxin (100 μM) and 6-cyano-2,3-dihydroxy-7- nitro-quinoxaline (10 μM) in the ACSF to block $GABA_A$ and AMPA receptor-

mediated synaptic currents, respectively. Each hemi-slice was used for a single experimental protocol depicted in the figure. All the drugs were dissolved in DMSO. The final concentration of DMSO was < 0.01%. Statistical significance was assessed using a paired t-test and one-way ANOVA for repeated-measures with significance for $p < 0.05$.

## 3. **Results**

### *3.1. COR758 failed to inhibit the [$^3$H]CGP54626 binding in rat cortical membranes*

To evaluate if COR758 (Fig 1A) binds to the orthosteric $GABA_B$ site, COR758 was characterized in a competition-binding assay using [$^3$H]CGP54626 and rat cortical membranes. CGP54626 completely inhibited the binding of [$^3$H]CGP54626 with an $IC_{50}$ of 2.7 ± 0.3 nM, while COR758 failed to displace [$^3$H]CGP54626 up to a concentration of 0.1 mM (Fig. 1B).

### *3.2. Molecular docking simulations showed that COR758 binds to an intrahelical allosteric binding site in the $GABA_{B1}$ subunit*

In the attempt to identify the possible binding site of COR758, molecular docking simulations were performed. The SiteMap routine (Halgren, 2009), which was applied to find putative binding sites for small molecule on the overall structure of the $GABA_BR$, led to the identification of four different binding regions (Fig. 2): (1) the orthosteric binding pocket that accommodated the CGP54626 antagonist on the VFT portion of the $GABA_{B1}$ monomer (Mao et al., 2020); (2) the allosteric interhelical site at the dimer interface; (3) two specular intrahelical binding regions where two [(2S)-3-[2-aminoethoxy(hydroxy)phosphoryl]oxy-2-[(Z)-octadec-9-enoyl]oxypropyl] octadecenoate molecules (https://pubchem.ncbi.nlm.nih.gov/compound/23727970) were located in the cryoEM structure of the inactive $GABA_B$ heterodimer at lower resolution (entry 6w2x of the protein data bank) (Papasergi-Scott et al., 2020).

Next, we performed molecular docking simulations to evaluate the ability of COR758 to bind each of the putative binding sites. Our compound showed a higher affinity (the docking score was -7

kcal/mol) for both the known allosteric binding sites (at the interhelical dimer interface and in the intrahelical space of the $GABA_{B2}$ monomer) than for the orthosteric site (-4 kcal/mol).

Interestingly, the binding region found in the $GABA_{B1a}$ monomer, which appeared specular to the intrahelical allosteric site in the $GABA_{B2}$ monomer, was predicted as the most probable binding site for COR758 (-9 kcal/mol). Tyr774 represented the major anchor point for our compound. In fact, phenyl ring of Tyr774 made π-π interactions with the aromatic scaffold of COR758 (Fig. 3), while a hydrogen bond was formed between the hydroxyl groups of the amino acid and our compound. Moreover, the $GABA_B$ receptor-COR758 complex was further stabilized by hydrophobic contacts between Leu667 and Leu725 and the isopropyl group at C6. The isopropyl group at C3 gave additional hydrophobic interactions with Ala837, Ala840, and Ile841. Finally, the N-alkyl chain was embedded into a hydrophobic region mainly defined by the aromatic portion of Phe674 and the alkyl portion of the Lys777 side chain. Similar results were obtained when COR758 was docked into the $GABA_{B1}$ monomer of the isoform 1b of $GABA_B$ starting from the cryo-EM structure 6wiv published by Park et al., 2020 and deposited in the protein data bank (https://www.rcsb.org/structure/6WIV) (data not shown). As COR758 occupied part of the $GABA_{B1}$ intrahelical binding site that also accommodated a long-chain lipophilic ligand in 6w2x, a cluster of hydrophobic interactions were common to COR758 and [(2S)-3-[2-aminoethoxy(hydroxy)phosphoryl]oxy-2-[(Z)-octadec-9-enoyl]oxypropyl] (Fig. 4).

Docking simulations therefore suggest that COR758 could occupy a newly allosteric binding site located in the intrahelical region of the $GABA_{B1}$ subunit.

### *3.3. Effect of COR758 on basal and $GABA_BR$-induced stimulation of [$^{35}$S]GTPγS binding*

We first examined the effects of COR758 on basal and $GABA_B$-stimulated activity using [$^{35}$S]GTPγS binding in rodent cortical membranes. As previously described (Mugnaini et al., 2020) and also shown in Fig. 5A COR758 significantly reduced basal [$^{35}$S]GTPγS binding to rat cortical membranes and this effect was also observed in the presence of the $GABA_BR$ competitive antagonist, CGP54626,

which had no effect by itself. GABA at 10 μM stimulated [$^{35}$S]GTPγS binding to approximately 125 ± 1.5% of basal activity and GABA-induced activation was antagonized by CGP54626 (Fig. 5B). COR758 significantly decreased GABA-stimulated [$^{35}$S]GTPγS binding in a concentration-dependent manner (5 and 25 μM); co-application with CGP54626 results in a synergistic inhibition of GABA-stimulated [$^{35}$S]GTPγS (Fig. 5B). To test whether COR758 alters the effect induced by the GS39783 on GABA-stimulated [$^{35}$S]GTPγS binding, we measured GABA-stimulated G protein activity in the presence of GS39783 and COR758 at 2.5 and 25 μM (Fig. 5C). Application of GS39783 (30 μM) increased GABA-induced [$^{35}$S]GTPγS binding to 167 ± 6.0%, an effect that was blocked by CGP54626. 25 μM COR758 significantly inhibited [$^{35}$S]GTPγS binding stimulated by GABA in the presence of GS39783 (Fig. 5C).

*3.4. COR758 inhibited the G protein dissociation induced by GABA and induces a conformational change between $GABA_{B1a}$ and $GABA_{B2}$ subunits*

To investigate the effect of COR758 on the $G\alpha_o$ protein subunit rearrangement mediated by $GABA_BR$ activation, we used BRET in CHO-$GABA_B$ cells co-expressing Gαo subunit fused to *Renilla reniformis* luciferase (Rluc) and the Gγ2 subunit fused to Venus. Basal and GABA-stimulated BRET was recorded in the presence or absence of COR758. As shown in Fig 6A, COR758 decreased the magnitude of BRET changes during GABA-induced G protein dissociation, thus leading to a decrease in ΔBRET at 25 μM compared to control (vehicle-treated) (Fig. 6B). Moreover, COR758 decreased, in a concentration-dependent manner, the rate of G protein dissociation, thereby increasing the time constant (tau) (Fig. 6C).

We then monitored the effect of COR758 on $GABA_BR$ subunit rearrangements (Geng et al., 2013; Xue et al., 2019), by measuring BRET in CHO cells transiently expressing $GABA_{B1a}$ fused to Rluc and $GABA_{B2}$ fused to YFP in the presence or absence of COR758 (Fig. 6D). In the absence of GABA, COR758 increased in a concentration-dependent manner basal BRET measured between $GABA_{B1a}$-Rluc and $GABA_{B2}$-YFP (Fig. 6E,F). GABA (100 μM) application, which induced a conformational

change within $GABA_BR$ subunits, resulted in a decrease in BRET (Fig. 6E). Finally, COR758 reduced GABA-induced $GABA_BR$ subunit rearrangement leading to a significant decrease in ΔBRET (Fig.6G).

*3.5. COR758 prevented GABA-mediated inhibition of adenylate cyclase activity.*

As COR758 inhibited $GABA_BR$-mediated $G_o$-protein activation, this compound is expected to inhibit $GABA_BR$ signalling pathways. In order to determine whether COR758 prevents $GABA_B$-mediated inhibition of adenylate cyclase activity, we measured intracellular cAMP formation in real time in CHO-$GABA_B$ cells transiently transfected with the CAMYEL sensor (Porcu et al., 2016, 2018). As expected, forskolin (0.5 µM) stimulated cAMP formation leading to a decrease in BRET (Fig. 7A). The addition of GABA reduced forskolin-stimulated cAMP production, as indicated by an increase in BRET (Fig. 7A). COR758 decreased in a concentration-dependent manner $GABA_BR$-mediated inhibition of adenylate cyclase activity, measured as a faster and enhanced CAMYEL activation compared to control, indicated by a significant decrease of ΔBRET (Fig. 7B) and the tau of CAMYEL activation (Fig. 7C).

*3.6. COR758 inhibited baclofen or CGP7930-induced ERK1/2 phosphorylation*

To explore the specificity of COR758 for $GABA_BR$ signaling, we analyzed phosphorylation of ERK1/2 in CHO-$GABA_B$ and CHO-D2 cells on Western blots. As the increase of ERK1/2 phosphorylation induced by $GABA_BR$ and D2 receptor activation is rapid and transient (Tu et al., 2007; Oak et al., 2000), we first incubated CHO-$GABA_B$ and CHO-D2 cells with baclofen/CGP7930 and dopamine/quinpirole, a dopamine D2-R agonist, respectively, at different time intervals. This step is needed to identify the time of the maximum increase of baclofen/CGP7930- and dopamine/quinpirole-induced ERK1/2 phosphorylation. As shown in Supplementary Figure 1A both baclofen (100 µM) and the ago-PAM CGP7930 (100 µM) (Tu et al., 2007; Chen et al., 2014) stimulated ERK1/2 phosphorylation in a time-dependent manner; baclofen-induced stimulation was

visible after 2.5 min and lasted up to 10 min, while CGP7930-induced stimulation was shorter, reaching the maximum after 2.5 min and returning to basal levels after 10 min incubation (Suppl. Fig. 1A). With CHO-$D_2$ cells, maximal dopamine-induced ERK phosphorylation was observed after 5 minutes, whereas quinpirole induced the maximum increase in ERK phosphorylation within 2.5 minutes (Suppl. Fig. 1B).

The increase in ERK1/2 phosphorylation by baclofen (100 μM) was completely prevented by preincubation with CGP54626 (100 μM), which had no effect by itself (Fig. 8A). In addition, CGP7930 alone at 100 μM (Fig. 8B) induces ERK1/2 phosphorylation, consistent with the reported ago-PAM activity (Chen et al., 2014). Pretreatment with COR758 (100 μM) blocked the effect of baclofen and CGP7930 on ERK1/2 phosphorylation (Fig. 8B).

To ascertain the selectivity of COR758 for $GABA_BR$, we tested whether this compound blocked quinpirole-induced phosphorylation mediated by the dopamine D2 receptor. As predicted, in CHO-D2 cells, quinpirole (1 μM) stimulated ERK1/2 phosphorylation, an effect that was abolished by pretreatment with the specific D2 receptor antagonist haloperidol (5 μM) (Fig. 8C). COR758 had no effect on D2 receptor-induced ERK1/2 activation and failed to inhibit quinpirole-induced ERK1/2 phosphorylation in CHO-D2 cells, demonstrating its specificity toward $GABA_BRs$ (Fig. 8D).

### *3.7. Fluorescent cell-based $Ca^{2+}$ mobilization assay in cell cultures*

#### *3.7. 1. Effects of COR758 on GABA- and baclofen-induced $Ca^{2+}$ mobilization*

We also investigated whether COR758 alters $GABA_BR$-induced intracellular $Ca^{2+}$mobilization in heterologous cells expressing a chimeric Gα protein artificially coupling the receptor to Gq signaling. GABA and baclofen concentration-dependently induced calcium transient in HEK293 stably expressing $GABA_{B1a}$ and $GABA_{B2}$ and the chimeric G protein, while COR758 was ineffective in mobilizing intracellular $Ca^{2+}$ (Fig.9). The $EC_{50}$ values of GABA and baclofen are shown in Table 1. To evaluate whether COR758 antagonizes GABA- and baclofen-induced $Ca^{2+}$ mobilization, concentration-response curves for GABA were built in either the absence or presence of COR758. At

the concentrations of 10 and 30 μM, but not 3 μM, our compound induced a significant rightward shift of the GABA concentration-response curve, thus increasing GABA $EC_{50}$ values, without a substantial change in the maximal response (Fig. 10A-C) (see also Table 1). COR758 at 30 μM also induced a significant rightward shift of baclofen concentration-response curve, thus increasing the baclofen $EC_{50}$ value to 273.0 ± 14.85 μM (Fig. 10D, Table 1).

*3.8 Synaptosome experiments*

*3.8.1 Effects of COR758 on glutamate efflux from rat frontal cortex and striatal synaptosomes*

In rat frontal cortex synaptosomes, a 90 sec pulse of a high $K^+$ concentration (15 mM) Krebs' solution significantly increased glutamate efflux (+58 ± 7%). This effect was significantly inhibited by addition of the $GABA_BR$ agonist baclofen (10 μM) to the perfusion medium, while COR758 (3 and 10 μM) had no effect (Fig. 11A). However, baclofen-induced reduction of $K^+$-evoked glutamate efflux was significantly inhibited by COR758 (10 μM). At the lower concentration tested (3 μM), COR758 failed to significantly modulate baclofen-induced reduction of $K^+$-evoked glutamate efflux from rat frontal cortex synaptosomes (Fig. 11A). Similar results were obtained by using striatal synaptosomes (Fig. 11B). At the concentrations tested, baclofen and COR758, alone or in combination, did not affect spontaneous glutamate efflux from rat frontal cortex synaptosomes (*data not shown*).

*3.8.2 Effects of quinpirole and COR758, alone or in combination, on glutamate efflux from rat striatum synaptosomes*

To further verify the selectivity of COR758 for $GABA_BR$, we evaluated its ability to alter quinpirole-induced inhibition of glutamate efflux from rat striatum synaptosomes. In rat striatum synaptosomes, the addition of the $D_2$ receptor agonist quinpirole (1 μM) to the perfusion medium, significantly inhibited the $K^+$-evoked glutamate efflux, while COR758 (3, 10 and 30 μM), by itself, had no effect. Moreover, at all concentration tested (3, 10 and 30 μM), COR758 failed to significantly modulate quinpirole-induced reduction of $K^+$-evoked glutamate efflux from rat striatal synaptosomes

(Fig.11C). At the concentrations tested, quinpirole and COR758, alone or in combination, did not affect spontaneous glutamate efflux from rat frontal cortex synaptosomes (*data not shown*).

*3.9. Effects of COR758 on baclofen-induced currents elicited by dopamine neurons ex vivo.*

We next performed whole-cell voltage-clamp ($V_{holding}$ = -70 mV) recordings from dopamine neurons in acute rat brain slices *ex vivo* to evaluate the effects of COR758 on baclofen-induced outward $K^+$ currents (Lacey et al., 1988; Jiang et al., 1993). As previously shown, bath application of baclofen (10 μM) induced an outward current (195.2 ± 19.31 pA; Fig. 12A) that is reproducible upon repeated applications over time (Porcu et al., 2018). However, when the slices were pretreated with COR758 (30 μM), the baclofen-induced outward current was prevented (10.02 ± 2.07 pA, Fig. 9A). The COR758 effect on baclofen-induced outward current is dose-dependent (Fig. 12B).

## 4. Discussion

In the present study, we report the *in vitro* characterization of the 4-hydroxy-2-quinolone derivative COR758, which acts as a $GABA_BR$ NAM in rat cortical membranes and in CHO and HEK293 cells stably expressing $GABA_BRs$. We confirm that COR758 inhibits basal and GABA-induced [$^{35}$S]GTPγS binding. Moreover, we demonstrate that this effect was also observed in the presence of the $GABA_BR$ antagonist and of the PAM GS39783, thus extending our previous data (Mugnaini et al., 2020). Of note, COR758 failed to displace [$^3$H]CGP54626 binding demonstrating that it does not directly interact with the orthosteric GABA binding site, but with an allosteric site.

Docking simulations showed that binding scores of COR758 interactions with the intrahelical allosteric site on $GABA_{B2}$ and with the allosteric site at the dimer interface were similar, which suggests that our compound binds to these regions in equilibrium, following a mode of binding similar to that previously shown for the positive allosteric modulator GS39783 (Shaye et al., 2020). However, COR758 showed the highest predicted affinity for a binding site on $GABA_{B1}$ that is specular to the intrahelical site on $GABA_{B2}$. Both sites can be physiologically occupied by an endogenous

phospholipid that was hypothesized to be a negative allosteric modulator of the $GABA_BR$ (Evenseth et al., 2020).

Accordingly, our docking studies suggest that the preferential binding region for COR758 might be an additional binding site for allosteric modulators. Interactions of COR758 with the $GABA_{B1}$ intrahelical pocket may displace or prevent binding of the endogenous phospholipid, thus stabilizing the receptor in an inactive state and disfavoring the interaction between $GABA_{B1}$ and ECL2 required for signal transduction. This intriguing finding warrants further investigations to characterize this intrahelical pocket as a new allosteric binding site.

In support of this hypothesis, in BRET experiments we showed that COR758 stabilizes the heterodimeric state of $GABA_{B1}$ and $GABA_{B2}$ subunits in the absence of GABA and prevents GABA-induced receptor subunit rearrangements. Interestingly, previous studies demonstrated that the ago-PAM CGP7930 induced a rearrangement of the transmembrane domains in the absence of agonist (Lecat-Guillet et al., 2017), suggesting that PAM and NAM compounds stabilize distinct $GABA_BR$ subunits conformations. All together, these data provide complementary information about the mode of action of COR758.

By monitoring the $G\alpha_o$ protein subunit rearrangement before and after $GABA_BR$ activation, we found that COR758 stabilizes the heterotrimeric state of the Go protein and prevents its conformational change induced by GABA application. These data suggest that COR758 affects $GABA_BR$ activation and basal activity by stabilizing a $GABA_BR$ conformation that prevents Gi/o protein activation and signaling to Gai/o effectors.

Indeed, we showed that COR758 acts as negative allosteric modulator of $GABA_BR$ in several functional assays, such as : ii) baclofen-induced decrease of cAMP production in transfected CHO-$GABA_B$ cells, iii) GABA- and baclofen-induced $Ca^{2+}$ mobilization in transfected HEK293 cells expressing a chimeric G protein; iv) baclofen-induced reduction of glutamate efflux from rat frontal cortex and striatal synaptosomes and vi) baclofen- and CGP7930-induced ERK1/2 phosphorylation.

In CHO-$GABA_B$ cells we found that COR758 prevented G protein-mediated $GABA_BR$ signaling to adenylyl cyclase, indicating that COR758 prevents Gαi/o protein signal pathway activation. COR758 also abolished both baclofen- and CGP7930-induced phosphorylation of ERK1/2, while it failed to inhibit ERK1/2 activation mediated by the D2 receptor, demonstrating its specificity/selectivity for $GABA_BRs$. COR758 also decreased, in a concentration-dependent manner, the intracellular free calcium [$Ca^{2+}$] release induced by GABA and baclofen in HEK-293 cells expressing $GABA_BR$ and a chimeric Gα protein, decreasing the potency of GABA without a substantial change in the GABA maximal response. These results suggest that the compound could act as a surmountable allosteric modulator [*i.e.*, allosteric modulators presenting a limiting value to the maximal displacement (Kenakin, 2009)]. However, further experiments are needed to confirm this hypothesis.

Considering the involvement of $GABA_BRs$ and the potential use of their ligands in CNS diseases (e.g., depression, cognition deficit, addiction, etc.), allosteric modulation of these receptors represents a promising approach for the treatment of several CNS disorders, offering the possibility of fine tuning $GABA_BR$ activity with improved pharmacological profiles. Indeed, COR758 prevents baclofen-induced reduction of $K^+$-evoked glutamate efflux from frontal cortex synaptosomes and fails to counteract quinpirole-induced reduction from striatal synaptosomes, suggesting its possible therapeutic use for glutamatergic dysfunction in mood disorders (Sanacora et al., 2012). By preventing baclofen-induced outward currents in VTA dopaminergic neurons COR758 may be also useful in mediating reward effects (Cruz et al., 2004). However, future studies are needed to explore the *in vivo* effects of COR758.

Despite $GABA_BR$ antagonists, which bind to the $GABA_BR$ orthosteric site, display a good bioavailability, high nanomolar affinity and can be orally administered (Iqbal and Gillani, 2016), their therapeutic use may induce unpredictable side effects. Previous studies showed that $GABA_BR$ antagonists are also allosteric modulators of the CXCL12 chemokine receptor CXCR4, expressed in the immune and nervous systems (Guyon et al., 2013). CXCR4 and $GABA_BRs$ often co-expressed in the same cell types (Banisadr et al., 2002), show complementary functionality and may be involved

in a cross talk (Duthey et al., 2010). For this reason, compounds such CGP55845 and CGP54626 *per se* can influence GABA transmission by the CXCR4 chemokine receptor.

PAMs and/or NAMs bind to allosteric binding sites, which show a lower degree of amino acid conservation relative to the orthosteric sites (Guyon et al., 2013), and exhibit improved target selectivity (Christopoulos, 2002; Lazareno et al., 2004). Importantly, allosteric modulation also increased chemical tractability (Nickols and Cohn, 2014). In spite of the greater receptor subtype-selectivity of allosteric respect to orthosteric ligands (Christopoulos, 2002; Lazareno et al., 1998, 2004; Nickols and Cohn, 2014), Hellyer et al. (2018) reported that GS39783 and CGP7930, previously classified as selective $GABA_BR$ allosteric modulators, displaced allosteric $mGlu_5$ radioligand [$^3$H]-methoxy-PEPy binding, consistent with a negative allosteric interaction on this receptor. COR758 structurally differs from known $GABA_BR$ PAM, potentially reducing off-target effects at mGluRs observed with other allosteric modulators. Further research is needed to determine potential off-target effects of COR758.

To date, there has been only one other reported $GABA_B$ NAM (CLH304a, Chen et al., 2014); it did not bind to the orthosteric binding sites of $GABA_B$ receptors but antagonize agonists and PAM-induced $GABA_B$-receptor signaling trough an allosteric binding site. A comparison of the effects induced by CLH304a and COR758 is reported in Table 1S.

Of note, additional comparative analysis of COR758 and the $GABA_B$ NAM CLH304a, using the web tool SwissADME [http://www.swissadme.ch], showed a higher ClogP (4.20 vs. 3.53) and a lower tPSA (42.23 Å vs. 74.60 Å) for COR758 suggesting a more favorable lipophilicity profile for our compound, which might facilitate blood-brain barrier penetration when administrated *in vivo*. The presence of an enolic OH generally reduces the susceptibility to conjugation with either glucuronic acid or sulfate, thus increasing the half-life of compounds, while the absence of the electrophilic α,ß-unsaturated ketone may improve the toxicological profile (Mugnaini and Corelli, 2016). A possibly improvement of pharmacokinetic/toxicological features of COR758 compared to CLH304a, however, needs to be confirmed in future studies.

The discovery and the characterization of a new compound acting as a $GABA_BR$ NAM offers advantages over previously reported antagonists in terms of selectivity, physicochemical properties and side effects. Overall, our findings indicate that COR758, a molecule with a different chemical structure, better lipophilicity and improved pharmacokinetic properties compared to other recently discovered $GABA_B$ NAMs might offer novel possibilities for therapeutic intervention with $GABA_BR$ signaling.

**Funding**

This work was supported by a grant from the Fondazione Banco di Sardegna to MPC (U1005-2014/AI.887

**CRediT authorship contribution statement**

**Alessandra Porcu:** Investigation, Formal Analysis, Writing – original draft. **Rafaela Mostallino:** Investigation, Formal Analysis, Writing – original draft. **Valeria Serra:** Investigation, Formal Analysis. **Miriam Melis:** Validation, Investigation, Formal Analysis. **Valeria Sogos:** Validation, Investigation, Formal Analysis. **Sarah Beggiato:** Investigation, Formal Analysis. **Luca Ferraro:** Validation, Investigation, Formal Analysis. **Bernard Bettler:** Writing – review & editing. **Fabrizio Manetti:** Conceptualization, supervision. **Beatrice Gianibbi**: investigation, formal analysis. **Federico Corelli:** Validation, Formal Analysis. **Claudia Mugnaini:** Conceptualization, Supervision, Writing – review & editing. **M Paola Castelli:** Conceptualization, Supervision, Writing – review & editing.

**Conflicts of interest**

The authors declare that they have no known competing financial interests or personal relationships that could have appeared to influence the work reported in this paper.

***References***

Agabio, R., Colombo, G., 2014. GABAB receptor ligands for the treatment of alcohol use disorder: preclinical and clinical evidence. Front Neurosci. 8, 140. https://doi.org/10.3389/fnins.2014.00140.

Agabio, R., Leite-Morris, K.A., Addolorato G., Colombo, G., 2016. Targeting the $GABA_B$ receptor for the treatment of alcohol use disorder, in: Colombo, G. (eds.), $GABA_B$ Receptor. The Receptors 29, Springer International Publishing, Cham, Switzerland, pp. 287-307. https://doi.org/10.1007/978-3-319-46044-4_15.

Banisadr, G., Fontanges, P., Haour, F., Kitabgi, P., Rostène, W., Mélik Parsadaniantz, S., 2002. Neuroanatomical distribution of CXCR4 in adult rat brain and its localization in cholinergic and dopaminergic neurons. Eur J Neurosci. 16, 1661-1671. https://doi.org/10.1046/j.1460-9568.2002.02237.x.

Beggiato, S., Borelli, A.C., Tomasini, M.C., Castelli, M.P., Pintori, N., Cacciaglia, R., Loche, A., Ferraro, L., 2018. In vitro functional characterization of GET73 as possible negative allosteric modulator of metabotropic glutamate receptor 5. Front Pharmacol. 9, 327. https://doi.org/10.3389/fphar.2018.00327.

Bettler, B., Kaupmann, K., Mosbacher, J., Gassmann, M., 2004. Molecular structure and physiological functions of GABA(B) receptors. Physiol Rev. 84, 835-867. https://doi.org/10.1152/physrev.00036.2003.

Binet, V., Brajon, C., Le Corre, L., Acher, F., Pin, J.P., Prézeau, L., 2004. The heptahelical domain of GABA(B2) is activated directly by CGP7930, a positive allosteric modulator of the GABA(B) receptor. J Biol Chem. 279, 29085-29091. https://doi.org/10.1074/jbc.m400930200.

Bowery, N.G., 2006. GABAB receptor: a site of therapeutic benefit. Curr Opin Pharmacol. 6, 37-43. https://doi.org/10.1016/j.coph.2005.10.002.

Bradford, M.M., 1976. A rapid and sensitive method for the quantitation of microgram quantities of protein utilizing the principle of protein-dye binding. Anal Biochem. 72, 248-254. https://doi.org/10.1016/0003-2697(76)90527-3.

Carai, M.A., Colombo, G., Froestl, W., Gessa, G.L., 2004. In vivo effectiveness of CGP7930, a positive allosteric modulator of the GABAB receptor. Eur J Pharmacol. 504, 213-216. https://doi.org/10.1016/j.ejphar.2004.10.008.

Castelli M.P., Casu, A., Casti, P., Lobina, C., Carai, M.A.M, Colombo, G., Solinas, M., Giunta, D., Mugnaini, C., Pasquini, S., Tafi, A., Brogi, S., Gessa, G.L., Corelli, F., 2012. Characterization of COR627 and COR628, two novel positive allosteric modulators of the GABA(B) receptor. J Pharmacol Exp Ther. 340, 529-538. https://doi.org/10.1124/jpet.111.186460.

Chen, L.H., Sun, B., Zhang, Y., Xu, T.J., Xia, Z.X., Liu, J.F., Nan, F.J., 2014. Discovery of a Negative Allosteric Modulator of GABAB Receptors. ACS Med Chem Lett. 5, 742-747. https://doi.org/10.1021/ml500162z.

Christopoulos, A., 2002. Allosteric binding sites on cell-surface receptors: novel targets for drug discovery. Nat Rev Drug Discov. 1, 198-210. https://doi.org/10.1038/nrd746.

Cruz, H.G., Ivanova, T., Lunn, M.L., Stoffel, M., Slesinger, P.A., Lüscher, C., 2004. Bi-directional effects of $GABA_B$ receptor agonists on the mesolimbic dopamine system. Nat Neurosci. 7, 153-159. https://doi.org/10.1038/nn1181.

Cryan, J.F., Kelly, P.H., Chaperon, F., Gentsch, C., Mombereau, C., Lingenhoehl, K., Froestl, W., Bettler, B., Kaupmann, K., Spooren, W.P.J.M., 2004. Behavioral characterization of the novel GABAB receptor-positive modulator GS39783 (N,N'-dicyclopentyl-2-methylsulfanyl-5-nitro-pyrimidine-4,6-diamine): anxiolytic-like activity without side effects associated with baclofen or benzodiazepines. J Pharmacol Exp Ther. 310, 952-963. https://doi.org/10.1124/jpet.104.066753.

Cryan, J.F., Kaupmann, K., 2005. Don't worry 'B' happy!: a role for GABA(B) receptors in anxiety and depression. Trends Pharmacol Sci. 26, 36-43. https://doi.org/10.1016/j.tips.2004.11.004.

de Beaurepaire, R., Sinclair, J.M.A., Heydtmann, M., Addolorato, G., Aubin, H.J., Beraha, E.M., Caputo, F., Chick, J.D., de La Selle, P., Franchitto, N., et al., 2019. The Use of Baclofen as a Treatment for Alcohol Use Disorder: A Clinical Practice Perspective. Front Psychiatry. 9, 708. https://doi.org/10.3389/fpsyt.2018.00708.

Dupuis, D.S., Relkovic, D., Lhuillier, L., Mosbacher, J., Kaupmann, K., 2006. Point mutations in the transmembrane region of GABAB2 facilitate activation by the positive modulator N,N'-dicyclopentyl-2-methylsulfanyl-5-nitro-pyrimidine-4,6-diamine (GS39783) in the absence of the GABAB1 subunit. Mol Pharmacol. 70, 2027-2036. https://doi.org/10.1124/mol.106.028183.

Duthey, B., Hübner, A., Diehl, S., Boehncke, S., Pfeffer, J., Boehncke, W.H., 2010. Anti-inflammatory effects of the GABA(B) receptor agonist baclofen in allergic contact dermatitis. Exp Dermatol. 19, 661-666. https://doi.org/10.1111/j.1600-0625.2010.01076.x.

Enna, S.J., McCarson, K.E., 2016. Targeting the GABAB receptor for the treatment of pain, in: Colombo, G. (eds.), GABAB Receptor. The Receptors 29, Springer International Publishing, Cham, Switzerland. https://doi.org/10.1007/978-3-319-46044-4_11.

Evenseth, L.S.M., Gabrielsen, M., Sylte, I., 2020. The GABAB receptor-structure, ligand binding and drug development. Molecules 25, 3093. https://doi.org/10.3390/molecules25133093.

Felice, D., O'Leary, O.F., Cryan, J.F., 2016. Targeting the GABAB receptor for the treatment of depression and anxiety disorders, in: Colombo, G. (eds.), GABAB Receptor. The Receptors 29, Springer International Publishing, Cham, Switzerland, pp. 219-250. https://doi.org/10.1007/978-3-319-46044-4_12.

Ferraro, L., Tanganelli, S., O'Connor, W.T., Bianchi, C., Ungerstedt, U., Fuxe, K., 1995. Neurotensin increases endogenous glutamate release in the neostriatum of the awake rat. Synapse. 20, 362-364. https://doi.org/10.1002/syn.890200409.

Ferraro, L., Beggiato, S., Marcellino, D., Frankowska, M., Filip, M., Agnati, L.F., Antonelli, T., Tomasini, M.C., Tanganelli, S., Fuxe, K., 2010. Nanomolar concentrations of cocaine enhance D2-like agonist-induced inhibition of the K+-evoked [3H]-dopamine efflux from rat striatal synaptosomes: a novel action of cocaine. J Neural Transm (Vienna). 117, 593-597. https://doi.org/10.1007/s00702-010-0389-4.

Frankowska, M., Filip, M., Przegaliński, E., 2007. Effects of GABAB receptor ligands in animal tests of depression and anxiety. Pharmacol Rep. 59, 645-655.

Frankowska, M., Przegaliński, E., Filip, M., 2016. Targeting the GABAB receptor for the treatment of substance use disorders, in: Colombo, G. (eds.), GABAB Receptor. The Receptors 29, Springer International Publishing, Cham, Switzerland, pp. 263-286. https://doi.org/10.1007/978-3-319-46044-4_14.

Froestl, W., Gallagher, M., Jenkins, H., Madrid, A., Melcher, T., Teichman, S., Mondadori, C.G., Pearlman, R., 2004. SGS742: the first GABA(B) receptor antagonist in clinical trials. Biochem Pharmacol. 68, 1479-1487. https://doi.org/10.1016/j.bcp.2004.07.030.

Froestl, W., 2010. Chemistry and pharmacology of GABAB receptor ligands. Adv Pharmacol. 58, 19-62. https://doi.org/10.1016/S1054-3589(10)58002-5.

Gambardella, A., Manna, I., Labate, A., Chifari, R., La Russa, A., Serra, P., Cittadella, R., Bonavita, S., Andreoli, V., LePiane, E., Sasanelli, F., Di Costanzo, A., Zappia, M., Tedeschi, G., Aguglia, U. Quattrone, A., 2003. GABA(B) receptor 1 polymorphism (G1465A) is associated with temporal lobe epilepsy. Neurology 60, 560-563. https://doi.org/10.1212/01.WNL.0000046520.79877.D8.

Gassmann, M., Bettler, B., 2012. Regulation of neuronal GABA(B) receptor functions by subunit composition. Nat Rev Neurosci. 13, 380–394. https://doi.org/10.1038/nrn3249.

Geng, Y., Bush, M., Mosyak, L., Wang, F., Fan, Q.R., 2013. Structural mechanism of ligand activation in human GABA(B) receptor. Nature. 504, 254-259. https://doi.org/10.1038/nature12725.

Guyon, A., Leresche, N., 1995. Modulation by different GABAB receptor types of voltage-activated calcium currents in rat thalamocortical neurones. J Physiol. 485, 29-42. https://doi.org/10.1113/jphysiol.1995.sp020710.

Guyon, A., Kussrow, A., Olmsted, I.R., Sandoz, G., Bornhop, D.J., Nahon, J.L., 2013. Baclofen and other GABAB receptor agents are allosteric modulators of the CXCL12 chemokine receptor CXCR4. J Neurosci. 33, 11643-11654. https://doi.org/10.1523/JNEUROSCI.6070-11.2013.

Halgren, T., 2009. Identifying and Characterizing Binding Sites and Assessing Druggability. J. Chem. Inf. Model. 49, 377-389. https://doi.org/10.1021/ci800324m

Hellyer, S.D., Albold, S., Wang, T., Chen, A.N.Y., May, L.T., Leach, K., Gregory, K.J., 2018. "Selective" Class C G Protein-Coupled Receptor Modulators Are Neutral or Biased $mGlu_5$ Allosteric Ligands. Mol Pharmacol. 93, 504-514. https://doi.org/10.1124/mol.117.111518.

Iqbal, F., Gillani, Q.A., 2016. GABAB receptor antagonists as cognition enhancers, in: Colombo, G. (eds.), $GABA_B$ Receptor. The Receptors 29, Springer International Publishing, Cham, Switzerland, pp. 377-385. https://doi.org/10.1007/978-3-319-46044-4_19.

Jacobson, L.H., Cryan J.F., 2008. Evaluation of the anxiolytic-like profile of the GABAB receptor positive modulator CGP7930 in rodents. Neuropharmacology. 54, 854-862. https://doi.org/10.1016/j.neuropharm.2008.01.004.

Jacobson, L.H., Vlachou, S., Slattery, D.A., Li, X., Cryan, J.F., 2018. The Gamma-Aminobutyric Acid B Receptor in Depression and Reward. Biol Psychiatry. 83, 963–976. https://doi.org/10.1016/j.biopsych.2018.02.006.

Jiang, Z.G., Pessia, M., North, R.A., 1993. Dopamine and baclofen inhibit the hyperpolarization-activated cation current in rat ventral tegmental neurones. J Physiol. 462, 753-764. https://doi.org/10.1113/jphysiol.1993.sp019580.

Jiang, L.I., Collins, J., Davis, R., Lin, K.M., DeCamp, D., Roach, T., Hsueh, R., Rebres, R.A., Ross, E.M., Taussig, R., Fraser, I., Sternweis, P.C., 2007. Use of a cAMP BRET sensor to characterize a novel regulation of cAMP by the sphingosine 1-phosphate/G13 pathway. J Biol Chem. 282, 10576-10584. https://doi.org/10.1074/jbc.m609695200.

Johnson, S.W., North, R.A., 1992. Two types of neurone in the rat ventral tegmental area and their synaptic inputs. J Physiol. 450, 455-468. https://doi.org/10.1113/jphysiol.1992.sp019136.

Kalinichev, M., Donovan-Rodriguez, T., Girard, F., Riguet, E., Rouillier, M., Bournique, B., Haddouk, H., Mutel, V., Poli, S., 2014. Evaluation of peripheral versus central effects of GABA(B) receptor activation using a novel, positive allosteric modulator of the GABA(B) receptor ADX71943, a pharmacological tool compound with a fully peripheral activity profile. Br J Pharmacol. 171, 4941-4954. https://doi.org/10.1111/bph.12812.

Kaupmann, K., Malitschek, B., Schuler, V., Heid, J., Froestl, W., Beck, P., Mosbacher, J., Bischoff, S., Kulik, A., Shigemoto, R., Karschin, A., Bettler, B., 1998. GABA(B)-receptor subtypes assemble into functional heteromeric complexes. Nature 396, 683-6. https://doi.org/10.1038/25360.

Kenakin, T., 2009. Allosteric drug antagonism, in: Kenakin, T. (eds.), A Pharmacology Primer-Theory, Application and Methods, 3rd Edn. Elsevier, Amsterdam, pp. 129-147. https://doi.org/10.1007/s00213-013-3226-2.

Koek, W., France, C.P., Cheng, K., Rice, K.C., 2010. GABAB receptor-positive modulators: enhancement of GABAB receptor agonist effects in vivo. J Pharmacol Exp Ther. 335, 163-171. https://doi.org/10.1124/jpet.110.171116.

Kulik, A., Vida, I., Fukazawa, Y., Guetg, N., Kasugai, Y., Marker, C.L., Rigato, F., Bettler, B., Wickman, K., Frotscher, M., Shigemoto, R., 2006. Compartment-dependent colocalization of Kir3.2-containing K+ channels and GABAB receptors in hyppocampal pyramidal cells. J. Neurosci. 26, 4289-4297. https://doi.org/10.1523/JNEUROSCI.4178-05.2006.

Lacey, M.G., Mercuri, N.B., North, R.A., 1988. On the potassium conductance increase activated by GABAB and dopamine D2 receptors in rat substantia nigra neurones. J Physiol. 401, 437-453. https://doi.org/10.1113/jphysiol.1988.sp017171.

Lazareno, S., Gharagozloo, P., Kuonen, D., Popham, A., Birdsall, N.J., 1998. Subtype-Selective Positive Cooperative Interactions between Brucine Analogues and Acetylcholine at Muscarinic

Receptors: Radioligand Binding Studies. Mol. Pharmacol. 53, 573-589. https://doi.org/10.1124/mol.53.3.573.

Lazareno, S., Dolezal, V., Popham, A., Birdsall, N. J. M., 2004. Thiochrome Enhances Acetylcholine Affinity at Muscarinic M4 Receptors: Receptor Subtype Selectivity via Cooperativity Rather than Affinity. Mol. Pharmacol. 65, 257-266. https://doi.org/10.1124/mol.65.1.257.

Lecat-Guillet, N., Monnier, C., Rovira, X., Kniazeff, J., Lamarque, L., Zwier, J.M., Trinquet, E., Pin, J.P., Rondard, P., 2017. FRET-based sensors unravel activation and allosteric modulation of the $GABA_B$ receptor. Cell Chem Biol. 24, 360-370. https://doi.org/10.1016/j.chembiol.2017.02.011.

Li, X., Risbrough, V.B., Cates-Gatto, C., Kaczanowska, K., Finn, M.G., Roberts, A.J., Markou, A., 2013. Comparison of the effects of the GABAB receptor positive modulator BHF177 and the GABAB receptor agonist baclofen on anxiety-like behavior, learning, and memory in mice. Neuropharmacology. 70, 156-167. https://doi.org/10.1016/j.neuropharm.2013.01.018.

Maccioni, P., Carai, M.A., Kaupmann, K., Guery, S., Froestl, W., Leite-Morris, K.A., Gessa, G.L., Colombo, G., 2009. Reduction of alcohol's reinforcing and motivational properties by the positive allosteric modulator of the GABA(B) receptor, BHF177, in alcohol-preferring rats. Alcohol Clin Exp Res. 33, 1749-1756. https://doi.org/10.1111/j.1530-0277.2009.01012.x.

Malherbe P, Masciadri R, Norcross RD, Knoflach, F., Kratzeisen, C., Zenner, M-T., Kolb, Y., Marcuz, A., Huwyler, J., Nakagawa, T., Porter, R.H.P., Thomas, A.W., Wettstein, J.G., Sleight, A. J., Spooren, W., Prinssen, E.P., 2008. Characterization of (R,S)-5,7-di-tert-butyl-3-hydroxy-3-trifluoromethyl-3H-benzofuran-2-one as a positive allosteric modulator of GABAB receptors. Br J Pharmacol. 154, 797-811. https://doi.org/10.1038/bjp.2008.135.

Mao, C., Shen, C., Li, C., Shen, D.-D., Xu, C., Zhang, S., Zhou, R., Shen, Q., Chen, L.-N., Jiang, Z., Liu, J., Zhang, Y., 2020. Cryo-EM structures of inactive and active $GABA_B$ receptor. Cell Res. 30, 564-573. https://doi.org/10.1038/s41422-020-0350-5.

Melis, M., Carta, S., Fattore, L., Tolu, S., Yasar, S., Goldberg, S.R., Fratta, W., Maskos, U., Pistis, M., 2010. Peroxisome proliferator-activated receptors-alpha modulate dopamine cell activity through nicotinic receptors. Biol Psychiatry. 68, 256-264. https://doi.org/10.1016/j.biopsych.2010.04.016.

Millan, M.J., 2002. Descending control of pain. Prog Neurobiol. 66, 355-474. https://doi.org/10.1016/S0301-0082(02)00009-6.

Millan, M.J., 2003. The neurobiology and control of anxious states. Prog Neurobiol. 70, 83-244. https://doi.org/10.1016/S0301-0082(03)00087-X.

Mombereau, C., Kaupmann, K., van der Putten, H., Cryan, J.F., 2004. Altered response to benzodiazepine anxiolytics in mice lacking GABA B(1) receptors. Eur J Pharmacol. 497, 119-120. https://doi.org/10.1016/j.ejphar.2004.06.036.

Mombereau, C., Kaupmann, K., Gassmann, M., Bettler, B., van der Putten, H., Cryan, J.F., 2005. Altered anxiety and depression-related behaviour in mice lacking GABAB(2) receptor subunits. Neuroreport. 16, 307-310. https://doi.org/10.1097/00001756-200502280-0002.

Mugnaini, C., Pedani, V., Casu, A., Lobina, C., Casti, A., Maccioni, P., Porcu, A., Giunta, D., Lamponi, S., Solinas, M., Dragoni, S., Valoti, M., Colombo, G., Castelli, M.P., Gessa, G.L., Corelli, F., 2013. Synthesis and pharmacological characterization of 2-(acylamino)thiophene derivatives as metabolically stable, orally effective, positive allosteric modulators of the GABAB receptor. J Med Chem. 56, 3620-3635. https://doi.org/10.1021/jm400144w.

Mugnaini, C., Corelli, F., 2016. The allosteric modulation of the GABAB receptor: a medicinal chemistry perspective, in: Colombo, G. (eds.), GABAB Receptor. The Receptors 29, Springer International Publishing, Cham, Switzerland, pp. 17-33. https://doi.org/10.1007/978-3-319-46044-4_3.

Mugnaini, C., Brizzi, A., Mostallino, R., Castelli, M.P., Corelli, F., 2020. Structure optimization of positive allosteric modulators of GABAB receptors led to the unexpected discovery of antagonists/potential negative allosteric modulators. Bioorg Med Chem Lett. 127443. https://doi.org/10.1016/j.bmcl.2020.127443.

Nakagawa, Y., Sasaki, A., Takashima, T., 1999. The GABA(B) receptor antagonist CGP36742 improves learned helplessness in rats. Eur J Pharmacol. 38, 1-7. https://doi.org/10.1016/S0014-2999(99)00567-1.

Nickols, H.H., Conn, P.J., 2014. Development of allosteric modulators of GPCRs for treatment of CNS disorders. Neurobiol Dis. 61, 55-71. https://doi.org/10.1016/j.nbd.2013.09.013.

Nowak, G., Partyka, A., Pałucha, A., Szewczyk, B., Wierońska, J. M., Dybała, M., Metz, M., Librowski, T., Froestl, W., Papp, M., Pilc, A., 2006. Antidepressant-like activity of CGP 36742 and CGP 51176, selective GABAB receptor antagonists, in rodents. Br J Pharmacol. 149, 581-590. https://doi.org/10.1038/sj.bjp.0706845.

Oak, J.N., Oldenhof, J., Van Tol, H.H., 2000. The dopamine D(4) receptor: one decade of research. Eur J Pharmacol. 405, 303-327. https://doi.org/10.1016/s0014-2999(00)00562-8.

Papasergi-Scott, M.M., Robertson, M.J., Seven, A.B., Panova, O., Mathiesen, J.M., Skiniotis, G., 2020. Structures of metabotropic GABAB receptor. Nature 584, 310-314. https://doi.org/10.1038/s41586-020-2469-4.

Park, H.W., Jung, H., Choi, K.H., Baik, J.H., Rhim, H., 2010. Direct interaction and functional coupling between voltage-gated CaV1.3 Ca2+ channel and GABAB receptor subunit 2. FEBS Lett. 584, 3317-3322. https://doi.org/10.1016/j.febslet.2010.07.014.

Park, J., Fu, Z., Frangaj, A., Liu, J., Mosyak, L., Shen, T., Slavkovich, V.N., Ray, K.M., Taura, J., Cao, B., Geng, Y., Zuo, H., Kou, Y., Grassucci, R., Chen, S., Liu, Z., Lin, X., Williams, J.P., Rice, W.J., Eng, E.T., Huang, R.K., Soni, R.K., Kloss, B., Yu, Z., Javitch, J.A., Hendrickson, W.A., Slesinger, P.A., Quick, M., Graziano, J., Yu, H., Fiehn, O., Clarke, O.B., Frank, J., Fan, Q.R., 2020. Structures of human $GABA_B$ receptor in an inactive state. Nature 584, 304-309. https://doi.org/10.1038/s41586-020-2452-0.

Paterson, N.E., Vlachou, S., Guery, S., Kaupmann, K., Froestl, W., Markou, A., 2008. Positive modulation of GABA(B) receptors decreased nicotine self-administration and counteracted nicotine-induced enhancement of brain reward function in rats. J Pharmacol Exp Ther. 326, 306-314. https://doi.org/10.1124/jpet.108.139204.

Pin, J.P., Prézeau, L., 2007. Allosteric modulators of GABA(B) receptors: mechanism of action and therapeutic perspective. Curr Neuropharmacol. 5, 195-201. https://doi.org/10.2174/157015907781695919.

Pin, J.P., Bettler, B., 2016. Organization and functions of mGlu and $GABA_B$ receptor complexes. Nature 540, 60–68. https://doi.org/10.1038/nature20566.

Porcu, A., Lobina, C., Giunta, D., Solinas, M., Mugnaini, C., Castelli, M.P., 2016. In vitro and in vivo pharmacological characterization of SSD114, a novel GABAB positive allosteric modulator. Eur J Pharmacol. 791, 115-123. https://doi.org/10.1016/j.ejphar.2016.08.032.

Porcu, A., Melis, M., Turecek, R, Ullrich, C., Mocci, I., Bettler, B., Gessa, G.L., Castelli, M.P., 2018. Rimonabant, a potent CB1 cannabinoid receptor antagonist, is a $G\alpha_{i/o}$ protein inhibitor. Neuropharmacology. 133, 107-120. https://doi.org/10.1016/j.neuropharm.2018.01.024.

Prosser, H.M., Gill, C.H., Hirst, W.D., Grau, E., Robbins, M., Calver, A., Soffin, E.M., Farmer, C.E., Lanneau, C., Gray, J., Schenck, E., Warmerdam, B.S., Clapham, C., Reavill, C., Rogers, D.C., Stean, T., Upton, N., Humphreys, K., Randall, A., Geppert, M., Davies, C.H., Pangaloset M.N., 2001. Epileptogenesis and enhanced prepulse inhibition in GABA(B1)-deficient mice. Mol Cell Neurosci. 17, 1059-1070. https://doi.org/10.1006/mcne.2001.0995.

Rajalu, M., Fritzius, T., Adelfinger, L., Jacquier, V., Besseyrias, V., Gassmann, M., Bettler, B., 2015. Pharmacological characterization of $GABA_B$ receptor subtypes assembled with auxiliary KCTD subunits. Neuropharmacology 88, 145–154. https://doi.org/10.1016/j.neuropharm.2014.08.020.

Roberts, D.C., Andrews, M.M., Vickers, G.J., 1996. Baclofen attenuates the reinforcing effects of cocaine in rats. Neuropsychopharmacology 15, 417-423. https://doi.org/10.1016/0893-133X(96)00002-4.

Sanacora, G., Treccani, G., Popoli, M., 2012. Towards a glutamate hypothesis of depression: an emerging frontier of neuropsychopharmacology for mood disorders. Neuropharmacology. 62, 63-77. https://doi.org/10.1016/j.neuropharm.2011.07.036.

Schuler, V., Lüscher, C., Blanchet, C., Klix, N., Sansig, G., Klebs, K., Schmutz, M., Heid, J., Gentry, C., Urban, L., Fox, A, Spooren, W., Jaton, A.L., Vigouret, J., Pozza, M., Kelly, P.H., Mosbacher, J., Froestl, W., Käslin, E., Korn, R., Bischoff, S., Kaupmann, K., van der Putten, H., Bettler, B., 2001. Epilepsy, hyperalgesia, impaired memory, and loss of pre- and postsynaptic GABA(B) responses in mice lacking GABA(B(1)). Neuron. 31, 47-58. https://doi.org/10.1016/S0896-6273(01)00345-2.

Schwenk, J., Metz, M., Zolles, G., Turecek, R., Fritzius, T., Bildl, W., Tarusawa, E., Kulik, A., Unger, A., Ivankova, K., Seddik, R., Tiao, J.Y., Rajalu, M., Trojanova, J., Rohde, V., Gassmann, M., Schulte, U., Fakler, B., Bettler, B., 2010. Native GABA(B) receptors are heteromultimers with a family of auxiliary subunits. Nature 465, 231-235. https://doi.org/10.1038/nature08964.

Shaye, H., Ishchenko, A., Lam, J.H., Han, G.W., Xue, L., Rondard, P., Pin, J.P., Katrich, V., Gati, C., Cherezov, V., 2020. Structural basis of the activation of a metabotropic GABA receptor. Nature 584, 298-303. https://doi.org/10.1038/s41586-020-2408-4.

Slattery, D.A., Desrayaud, S., Cryan, J.F., 2005. GABAB receptor antagonist-mediated antidepressant-like behavior is serotonin-dependent. J Pharmacol Exp Ther. 312, 290-296. https://doi.org/10.1124/jpet.104.073536.

Sun, B., Chen, L., Liu, L., Xia, Z., Pin, J.P., Nan, F., Liu, J., 2016. A negative allosteric modulator modulates GABAB-receptor signalling through GB2 subunits. Biochem J. 473, 779-787. https://doi.org/10.1042/BJ20150979.

Tao, R., Auerbach, S.B., 2002. GABAergic and glutamatergic afferents in the dorsal raphe nucleus mediate morphine-induced increases in serotonin efflux in the rat central nervous system. J Pharmacol Exp Ther. 303, 704-710. https://doi.org/10.1124/jpet.102.038133.

Tu, H., Rondard, P., Xu, C., Bertaso, F., Cao, F., Zhang, X., Pin, J.P., Liu, J., 2007. Dominant role of GABAB2 and Gbetagamma for GABAB receptor-mediated-ERK1/2/CREB pathway in cerebellar neurons. Cell Signal. 19, 1996-2002. https://doi.org/10.1016/j.cellsig.2007.05.004.

Turecek, R., Schwenk, J., Fritzius, T., Ivankova, K., Zolles, G., Adelfinger, L., Jacquier, V., Besseyrias, V., Gassmann, M., Schulte, U., Fakler, B., Bettler, B., 2014. Auxiliary GABAB receptor subunits uncouple G protein βγ subunits from effector channels to induce desensitization. Neuron 82, 1032–1044. https://doi.org/10.1016/j.neuron.2014.04.015.

Urwyler, S., Mosbacher, J., Lingenhoehl, K., Heid, J., Hofstetter, K., Froestl, W., Bettler, B., Kaupmann, K., 2001. Positive allosteric modulation of native and recombinant gamma-aminobutyric acid(B) receptors by 2,6-Di-tert-butyl-4-(3-hydroxy-2,2-dimethyl-propyl)-phenol (CGP7930) and its aldehyde analog CGP13501. Mol. Pharmacol. 60, 963–971. https://doi.org/10.1124/mol.60.5.963.

Urwyler, S., Pozza, M.F., Lingenhoehl, K., Mosbacher, J., Lampert, C., Froestl, W., Koller, M., Kaupmann, K., 2003. N,N′-Dicyclopentyl-2-methylsulfanyl-5-nitro-pyrimidine-4,6-diamine (GS39783) and structurally related compounds: novel allosteric enhancers of gamma-aminobutyric acidB receptor function. J Pharmacol Exp Ther. 307, 322–330. https://doi.org/10.1124/jpet.103.053074.

Urwyler, S., 2011. Allosteric modulation of family C G-protein-coupled receptors: from molecular insights to therapeutic perspectives. Pharmacol Rev. 63, 59–126. https://doi.org/10.1124/pr.109.002501.

Urwyler, S., 2016. Allosteric Modulators: The New Generation of $GABA_B$ Receptor Ligands, in: Colombo, G. (eds), $GABA_B$ Receptor. The Receptors 29, Humana Press, Cham, pp. 357-375. https://doi.org/10.1007/978-3-319-46044-4_18.

Xue, L., Sun, Q., Zhao, H., Rovira, X., Gai, S., He, Q., Pin, J.P., Liu, J., Rondard, P., 2019. Rearrangement of the transmembrane domain interfaces associated with the activation of a GPCR hetero-oligomer. Nat Commun. 10, 2765. https://doi.org/10.1038/s41467-019-10834-5.

Zheng, S., Abreu, N., Levitz, J., Kruse, A. C., 2019. Structural basis for KCTD-mediated rapid desensitization of $GABA_B$ signalling. Nature 567, 127-131. https://doi.org/10.1038/s41586-019-0990-0.

**Figure Legends**

**Figure 1. Chemical structure of 4-hydroxy-1-isobutyl-3, 6-diisopropylquinolin-2(1*H*)-one (COR758) (A); Displacement curves of [$^3$H]CGP54626 by COR758 (←) and CGP54626 (●) in rat cortical membranes (B)** Cortical rat membranes were incubated in the presence of 3 nM of [$^3$H]CGP54626 (85 Ci/mM) with serial dilutions ranging from $10^{-10}$ to $10^{-7}$ or $10^{-10}$ to $10^{-4}$ M of unlabelled CGP54626 or COR758, respectively. Data represent a typical experiment out of three independent experiments, expressed as percentage of specific binding. The calculation of $IC_{50}$ was performed by non-linear curve fitting of the concentration-effect curves using the Graph Pad Prism Program. The F-test was used to determine the best approximation of a non-linear curve fitting to one or two site model ($p < 0.05$).

**Figure 2. Graphical representation of the putative binding sites found by SiteMap on the structure of $GABA_BR$** (entry 7c7s of the protein data bank). Four regions were identified: the orthosteric binding site in the $GABA_{B1a}$ monomer (red) that accommodate the antagonist CGP54626 (yellow); the interhelical allosteric site between $GABA_{B1}$ and $GABA_{B2}$ subunits (white); the intrahelical allosteric binding site in $GABA_{B2}$ (blue); an additional intrahelical binding site in the $GABA_{B1}$ specular to the intrahelical allosteric site in the $GABA_{B2}$ (green).

**Figure 3. Schematic representation of the interaction pattern of COR758 with the interhelical binding site within the $GABA_{B1a}$ subunit.** Tyr774 is the anchor point for the ligand, making a hydrogen bond (white dashed line) with the C4 hydroxyl group of COR758, as well as π-π interactions (yellow dashed lines) with the aromatic core of the ligand. Extensive hydrophobic contacts also involve the alkyl substituents of COR758 and the receptor. For the sake of clarity, only a few amino acids, important for ligand binding, are reported.

**Figure 4. Schematic representation of the interaction pattern of COR758 with the interhelical binding site within the $GABA_{B1}R$ subunit.** Comparison of the allosteric intrahelical binding site found in the $GABA_{B1}R$ subunits of cryo-EM $GABA_B$ complexes stored as 7c7s and 6w2x in the protein data bank, respectively. The structure of COR758 (thick stick atom type notation) and the [(2*S*)-3-[2-aminoethoxy(hydroxy)phosphoryl]oxy-2-[(*Z*)-octadec-9-enoyl]oxypropyl] octadecenoate (green) are also reported to show that COR758 can occupy part of the binding site of the long-chain hydrophobic ligand.

**Figure 5. Effects of COR758 on basal and $GABA_B$ induced stimulation of [$^{35}$S]GTPγS binding in rat frontal cortex membranes**. COR758 was tested alone or in combination with the competitive antagonist of the $GABA_BR$, CGP54626 (A), GABA or GABA + CGP54626 (B) and the $GABA_B$ PAM GS39783 (C). Data represent the mean ± S.E.M. calculated from at least three independent experiments performed in triplicate, and expressed as percentage of basal activity, binding in the absence of ligands being defined as 100%. Horizontal dotted lines indicate baseline values and the degree of stimulation with agonist alone, respectively. (A) One-way ANOVA: $F(7,28) = 41.36$, $p<0.0001$; *p< 0.05 **p< 0.01 and ***p< 0.001 with respect to basal values, Tukey's test. (B) One-way ANOVA: $F(8,47) = 40.09$, $p<0.0001$; ***p< 0.001 with respect to basal values, $^{###}p<0.001$ with respect to GABA, $^{°°}p< 0.01$ and $^{°°°}p<0.001$ with respect to GABA + COR758 2.5 µM and GABA + COR758 5 µM respectively, Tukey's test. (C) One-way ANOVA: $F(6,18) = 31.49$, $p<0.0001$; **p< 0.01 and ***p< 0.001 with respect to basal values, $^{+}p<0.05$, $^{++}p<0.01$ with respect to GABA, $^{###}p<0.001$ with respect to GABA+GS, Tukey's test. COR, COR 758; CGP, CGP54626; GS, GS39783.

**Figure 6. Effects of COR758 on G protein dissociation and on $GABA_{B1a}$ and $GABA_{B2}$ subunits rearrangement.** (A) BRET kinetics in CHO-$GABA_B$ expressing Gαo-Rluc and $G\gamma_2$–Venus

measured in the absence (●) and presence of COR758 (● 25 µM). Injection of 100 µM GABA induced changes in BRET signal due to conformational rearrangement between Gαo-Rluc and $G\gamma_2$–Venus subunits. The curves were fitted with Plateau followed by one-phase decay equation, the data are expressed in mBRET units (change in BRET ratio x 1000). (B) Bar graph showing the change in ΔBRET determined in experiments as in (A). Data are presented as a mean ± SEM of 3 independent experiments. One-way ANOVA: $F(3,8) = 2.97$, $p=0.09$, *$p<0.05$, vs GABA, Bonferroni test. (C) Bar graph showing the amplitude-weighted mean time constant (tau dissociation) obtained by fitting BRET recovery phase to a double exponential function. Data are presented as a mean ± SEM of 3 independent experiments. One-way ANOVA: $F(3,8) = 12$, $p<0.01$; *$p<0.05$, **$p<0.01$ vs GABA, Bonferroni test. COR, COR758. (D) Cartoon illustrating the Rluc probe (red) inserted in the C-terminal of $GABA_{B1a}$ subunit and YFP (green) probe inserted in the C-terminal of $GABA_{B2}$ subunit. (E) BRET kinetics measured in the absence (●) and presence of COR758 (● 25 µM). Injection of 100 µM GABA induced changes in BRET signal due to conformational rearrangement between $GABA_{B1a}$-Rluc and $GABA_{B2}$-YFP subunits. The curves were fitted with Plateau followed by one-phase decay equation, the data are expressed in mBRET units (change in BRET ratio x 1000). (F) Bar graph showing the change in basal BRET determined in experiments as in (E). Data are presented as a mean ± SEM of 5 independent experiments. One-Way ANOVA $F(3,16) = 21.43$, $p<0.001$; *$p<0.05$, **$p<0.01$, ***$p<0.001$ vs Control, Bonferroni test. (G) Bar graph showing the change in ΔBRET determined in experiments as in (E). Data are presented as a mean ± SEM of 5 independent experiments. One-way ANOVA: $F(3,16) = 11.88$, $p<0.001$; **$p<0.01$, ***$p<0.001$ vs GABA, Bonferroni test. CTR, Control; COR, COR758.

**Figure 7. Effects of COR758 on GABA-inhibition of Adenylate Cyclase activity.** (A) BRET kinetics measured in the absence (●) and presence of COR758 (● 25 µM) in CHO-$GABA_B$ cells transiently co-expressing CAMYEL sensor. 0.5 µM Forskolin was injected after 19 cycles (~100 sec) of reading, GABA 10 µM was injected after 99 cycles (~380 sec). Data are the means ± SEM of

triplicate determinations from a representative experiment. (B) Bar graph showing the change in ΔBRET determined in experiments as in (A). Data are presented as a mean ± SEM of 5 independent experiments, performed in triplicate. One-way ANOVA: $F(3,12) = 11.36$, $p<0.001$; *$p<0.05$ **$p<0.01$, ***$p<0.001$ vs GABA, Bonferroni test. (C) Bar graph showing the amplitude-weighted mean time constant (tau CAMYEL activity) obtained by fitting BRET recovery phase to a double exponential function. Data are presented as a mean ± SEM of 5 independent experiments. One-way ANOVA: $F(3,12) = 11.91$, $p<0.001$; **$p<0.01$, ***$p<0.001$ vs GABA, Bonferroni test. COR, COR758.

**Figure 8. COR758 specifically inhibits baclofen and CGP7930-induced ERK1/2 phosphorylation.** (A) Baclofen (100 μM) induces ERK1/2 phosphorylation in CHO-$GABA_B$ cells that is inhibited by the antagonist CGP54626 (100 μM). One-way ANOVA: $F(3,12) = 14.43$, $p=0.0004$, **$p< 0.01$ with respect to basal values, and $^{###}p< 0.001$ versus baclofen + CGP54626, Newman-Keuls test. (B) Inhibitory effect of COR758 (100 μM) on baclofen and CGP7930 (100 μM) -induced ERK1/2 phosphorylation in CHO-$GABA_B$ cells. One-way ANOVA: $F(5,18) = 9.79$, $p= 0.0001$, *$p<0.05$, ***$p<0.001$, with respect to basal values; $^{###}p< 0.001$ versus baclofen + COR758 and °$p< 0.05$ versus CGP7930 + COR758, Newman-Keuls test. (C) Quinpirole (1 μM) induces ERK1/2 phosphorylation in CHO-$D_2$ cells that is inhibited by the antagonist haloperidol (5 μM). One-way ANOVA: $F(3,8) = 34.64$, $p=0.0001$, ***$p<0.001$ with respect to basal values, and $^{###}p< 0.001$ versus quinpirole + haloperidol, Newman-Keuls test. (D) COR758 has no effect on quinpirole-induced ERK1/2 phosphorylation in CHO-$D_2$ cells. One-way ANOVA: $F(7,16) = 77.60$, $p=0.0001$, ***$p<0.001$ with respect to basal values, Newman-Keuls test. Data are presented as a mean ± SEM of 3 independent experiments. COR, COR758.

**Figure 9. GABA, baclofen and COR758 concentration-response curves in HEK293 stable cell line co-expressing the two subunits of the human $GABA_BR$, GABAB1(a) and GABAB2, with a**

**chimeric Gα protein allowing redirection of receptor activation onto calcium signalling**. The effects of the treatments on intracellular calcium levels are expressed as % of maximal response over the basal values. Concentration-response curves were generate using non-linear regression [curve fit, log(agonist) vs. response, variable slope, four parameters]. Each point represents the mean ± SEM (n = 3). The compound $EC_{50}$ values are provided in Table 1. Bacl, Baclofen; COR, COR 758.

**Figure 10. Effects of COR758 (3-30 µM) on GABA (*Panels A-C*) and baclofen (*Panel D*) concentration-dependent increase in intracellular calcium levels in HEK293 stable cell line co-expressing the two subunits of the human $GABA_BR$, $GABA_{B1(a)}$ and $GABA_{B2}$, with a chimeric Gα protein allowing redirection of receptor activation onto calcium signaling**. The effects of the treatments on intracellular calcium levels are expressed as % of maximal response over the basal values. Each point represents the mean ± SEM (n = 4). Concentration-response curves were generate using non-linear regression [curve fit, log(agonist) vs. response, variable slope, four parameters]. GABA or Baclofen $EC_{50}$ values under the different experimental conditions are provided in Table 1. COR, COR 758; bacl, baclofen.

**Figure 11. Effects of baclofen (10 µM; *Panels A and B*) or quinpirole (1 µM; *Panel C*) and COR758 (3 and 10 µM), alone and in combination, on of $K^+$ evoked glutamate efflux from rat frontal cortex (*Panels A*) or striatal (*Panels B and C*) synaptosomes.** The drugs were added alone or in combination concomitantly with the depolarizing stimulus (15 mM, $K^+$, 90 s). A same volume of vehicle (Kreb's solution) was combined to the depolarizing stimulus in the control groups. The effect of the treatments on $K^+$-evoked glutamate efflux is expressed as percent of control values (*Panel A* = 100 ± 4%, n = 14; *Panel B* = 100 ± 5%, n = 14; *Panel C* = 100 ± 3%, n = 14; indicated by the dashed lines) *i.e.* $K^+$-evoked glutamate efflux measured in untreated synaptosomes, always assayed in parallel. Each treatment bar represents the mean ± SEM of 5-7 determinations run in duplicate. Panel A: One-way ANOVA: $F(5,20) = 37.43$, $p<0.0001$, $^{**}p < 0.01$ significantly different

from the respective control (*i.e.* 100%) as well as COR alone groups, Newman-Keuls test; Panel B: One-way ANOVA: $F(5,24) = 31.65$, $p<0.0001$, $^{**}p < 0.01$ significantly different from the respective control (*i.e.* 100%) as well as COR alone groups, Newman-Keuls test; Panel C: One-way ANOVA: $F(7,39) = 32.08$, $p<0.0001$, $^{**}p<0.01$ significantly different from the respective control (*i.e.* 100%) as well as COR alone groups, Newman-Keuls test. Bacl, baclofen; COR, COR 758; Quin, quinpirole.

**Figure 12. Effect of COR758 on outward currents evoked by $GABA_BR$ activation on rat dopamine neuron. (A)** Graph illustrates the time course of the average effects of baclofen (10 μM) and COR758 (30 μM) on the holding current ($I_{hold}$) recorded from dopamine cells *ex vivo*. When baclofen (grey bar) is bath applied, a voltage-clamped ($V_{holding}$= - 70 mV) rat dopamine neuron elicits an outward current that is reproducible over time unless COR758 is applied before (black bar). All data are normalized to the respective baseline current (5 min). Grey and black bars show the time of superfusion of bacl and COR. SEM bars are smaller than symbols in some cases. Bath application of baclofen (10 μM) induced an outward current of 195.2 ± 19.31 pA, n=4; the baclofen-induced outward current was prevented in the presence of COR758 at 30 μM (10.02 ± 2.07 pA, n= 4; p=0.0024, paired *t* test, $t_4$=3,53). **(B)** Dose-response relationship shows the effect of COR758 on baclofen-induced outward current. COR758 3-30 μM; n= 4 per group; One-way ANOVA followed by Dunnett's test, $F(3,12) = 37.31$, $^{**}p<0.01$, $^{***}p< 0.001$, $^{****}p< 0.0001$. Bacl, baclofen; COR, COR758.

**Supplemental Figure 1.** Time course of ERK1/2 phosphorylation induced by $GABA_B$ or D2 receptor activation. Effect of baclofen and CGP7930 (A), dopamine and quinpirole (B) in the increase of ERK1/2 phosphorylation in CHO-$GABA_B$ and CHO-D2 cells, respectively. Cells were treated with baclofen (100 μM ) or with CGP7930 (100 μM) (A) or with dopamine (1 μM) or quinpirole (1 μM ) (B) for up 10 min; after drug incubation total (ERK1/2) and phosphoERK1/2 (p-

ERK1/2) was detected by western blot. Data represent a typical experiment out of three independent experiments.

**Supplemental Figure 2.** Untruncated image of the blots shown in Supplemental Fig. 1 A-B and in Fig. 6 A-D.

**Table 1.** $EC_{50}$ values obtained with GABA and glutamate in the absence or in the presence of COR758 (COR; 3-30 μM) by evaluating intracellular calcium levels.

| Compound(s) | EC50 (μM) |
|---|---|
| GABA | 14.31 ± 1.36 |
| BACLOFEN | 8.68 ± 1.67 |
| COR | n.d. |
| | |
| GABA + COR 3 μM | 12.12 ± 0.46 |
| GABA + COR 10 μM | 78.77 ± 8.51** |
| GABA + COR 30 μM | 246.8 ± 18.74** |
| BACLOFEN + COR 30 μM | 273.4 ± 14.85°°° |

Intracellular calcium levels have been measured in HEK293 stable cell line co-expressing the two subunits of the human GABABR, GABAB1(a) and GABAB2, with a chimeric Gα protein allowing redirection of receptor activation onto calcium signalling. Results are expressed as mean ± S.E.M. of 4 independent experiments. $EC_{50}$ values were calculated using non-linear regression [curve fit, log(agonist) vs response, variable slope, four parameters]. Statistical differences between group means for $EC_{50}$ values were also assessed by ANOVA followed by Tukey's multiple comparisons test. **$p<0.01$, significantly different from GABA; °°$p<0.01$, significantly different from BACLOFEN.

## Table1S: Main properties of COR758 and CLH303A: common features.

| | CLH304a | COR758 |
|---|---|---|
| *[$^3$H]CGP54626 binding* | No binding to orthosteric binding site | No binding to the orthosteric binding site |
| *Intracellular calcium measurement* | Inhibition of GABA-, APPA- or Baclofen-induced $Ca2^+$ release in HEK293-GB1+GB2 and in CGNs. | Inhibition of GABA or -Baclofen-induced $Ca2^+$ release in HEK293-GB1+GB2 |
| *ERK1/2 Phosphorylation* | Inhibition of Baclofen or CGP7930-induced ERK1/2 phosphorylation in HEK293- GB1+GB2 or in CGNs | Inhibition of Baclofen or CGP7930 induced ERK1/2 phosphorylation in CHO-GABA-GB1+GB2 |

Abbreviations: APPA, 3aminopropanephoshinic acid; CGNs, cultured cerebellar granular neurons; HEK293-GB1+GB2, human embryonic kidney overexpressing $GABA_B$ receptor subunits (GB1 and GB2).

**Figure 1**

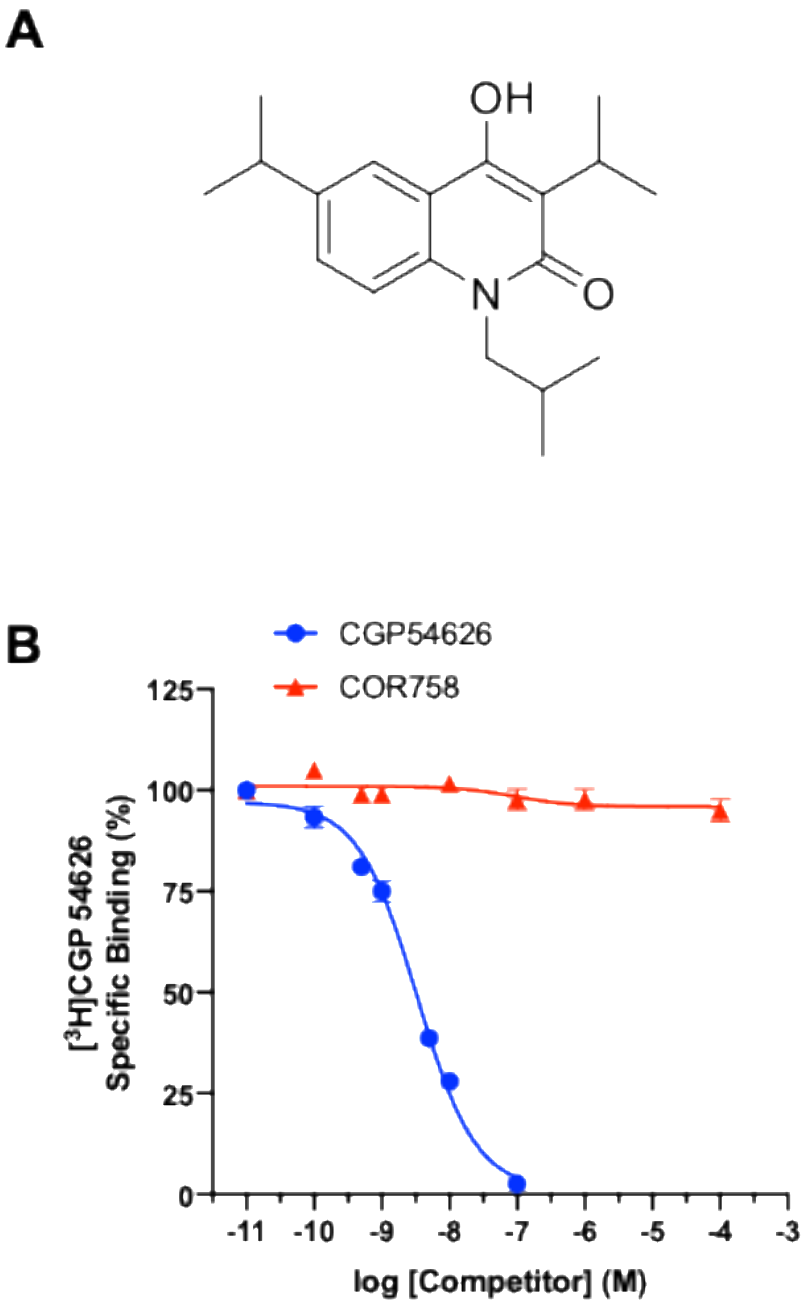
A
OH
N
O
B
CGP54626
COR758
125
100
75
50
25
0
[3H]CGP 54626
Specific Binding (%)
-11
-10
-9
-8
-7
-6
-5
-4
-3
log [Competitor] (M)

**Figure 2**

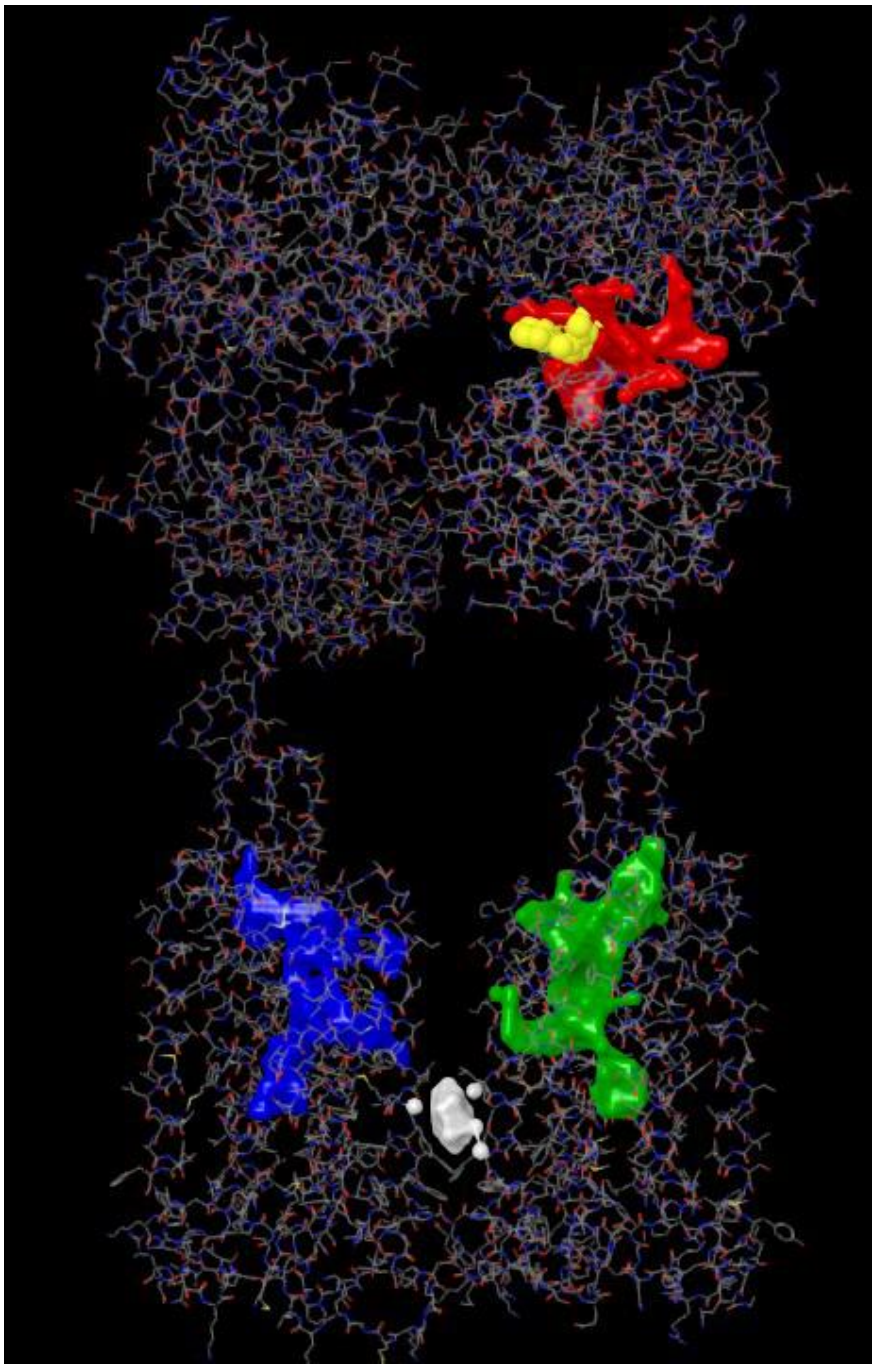

**Figure 3**

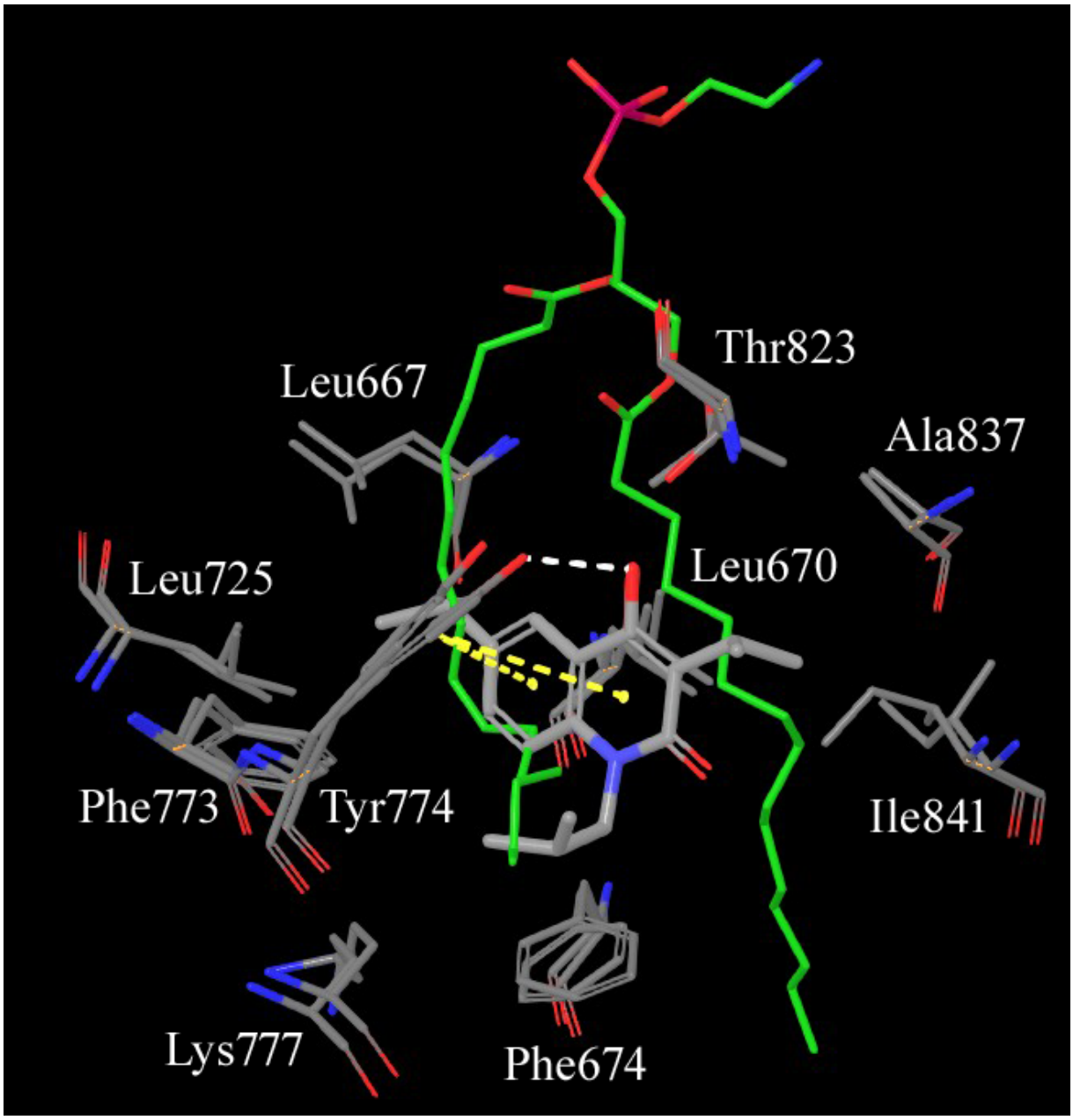
Thr823
Leu667
Ala837
Leu725
Leu670
Phe773
Tyr774
Ile841
Lys777
Phe674

**Figure 4**

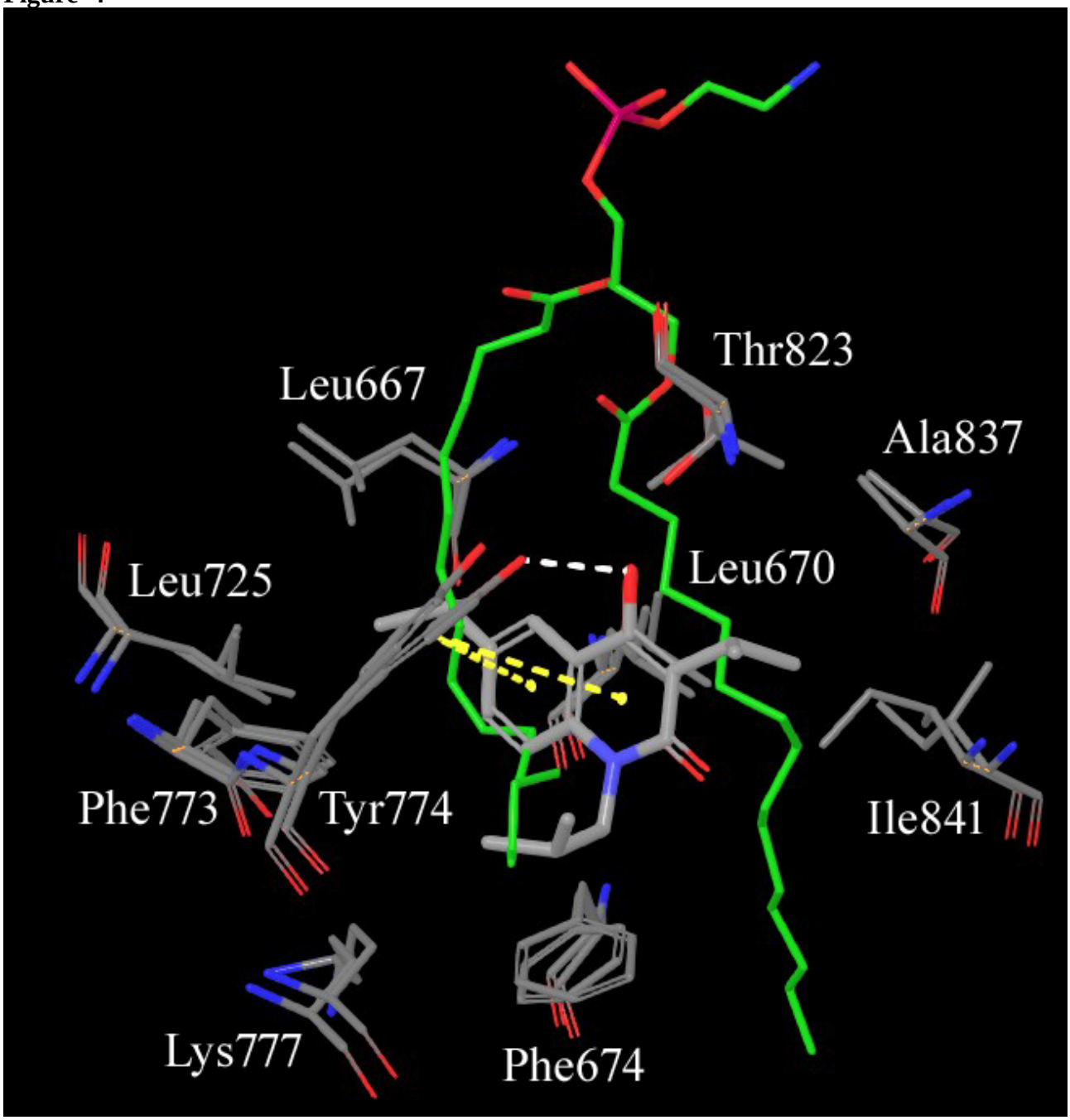
Thr823
Leu667
Ala837
Leu725
Leu670
Phe773
Tyr774
Ile841
Lys777
Phe674

**Figure 5**

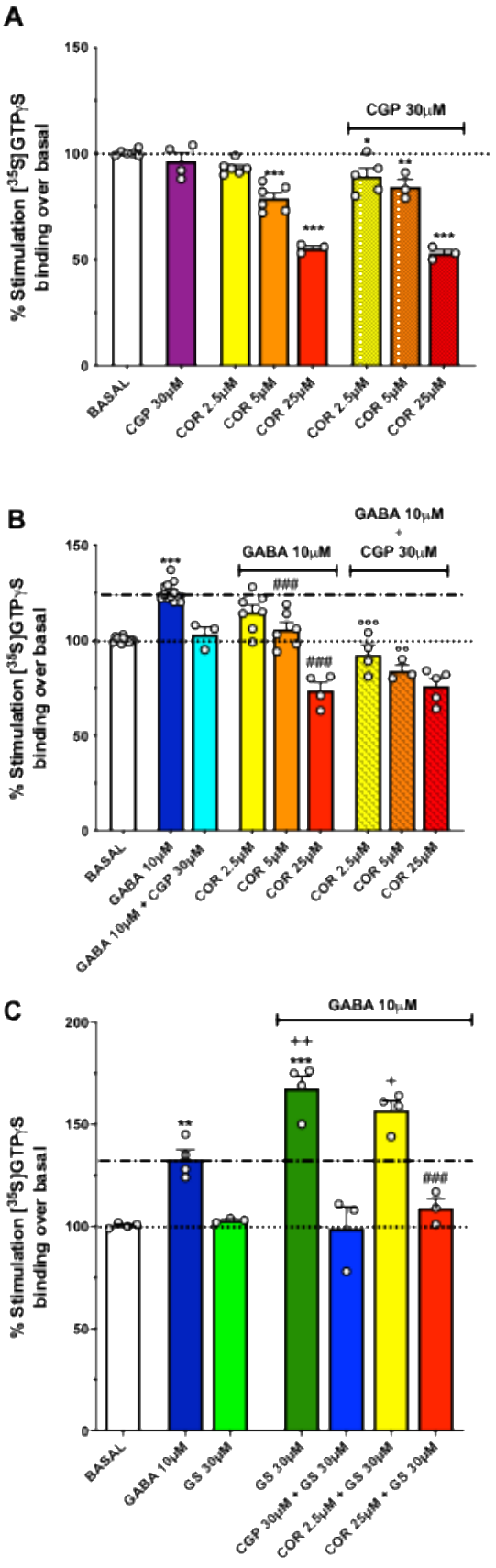
A
% Stimulation [35S]GTPγS binding over basal
CGP 30µM
BASAL
CGP 30µM
COR 2.5µM
COR 5µM
COR 25µM
B
GABA 10µM + CGP 30µM
GABA 10µM
GABA 10µM + CGP 30µM
C
GABA 10µM
BASAL
GABA 10µM
GS 30µM
GS 30µM
CGP 30µM + GS 30µM
COR 2.5µM + GS 30µM
COR 25µM + GS 30µM

**Figure 6**

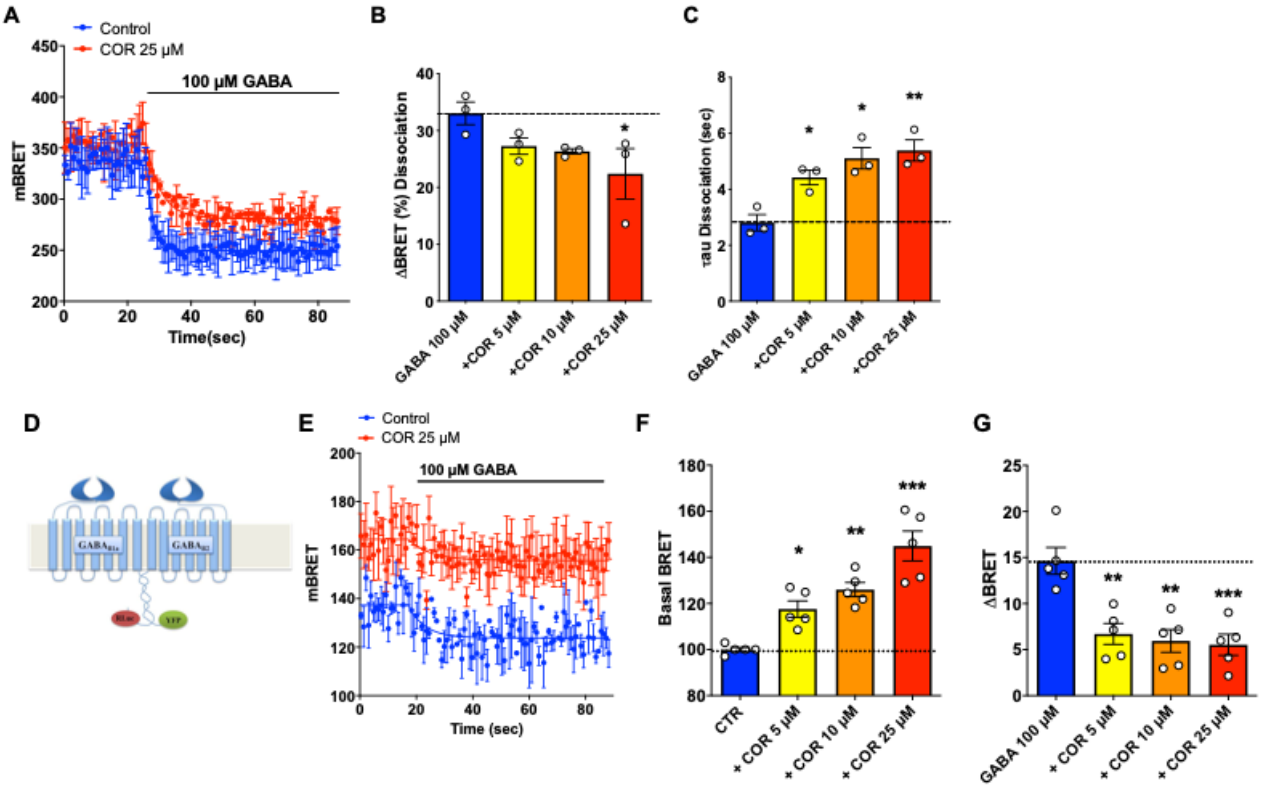
A
Control
COR 25 µM
100 µM GABA
mBRET
Time(sec)
B
ΔBRET (%) Dissociation
GABA 100 µM
+COR 5 µM
+COR 10 µM
+COR 25 µM
C
τau Dissociation (sec)
GABA 100 µM
+COR 5 µM
+COR 10 µM
+COR 25 µM
D
E
Control
COR 25 µM
100 µM GABA
mBRET
Time (sec)
F
Basal BRET
CTR
+ COR 5 µM
+ COR 10 µM
+ COR 25 µM
G
ΔBRET
GABA 100 µM
+ COR 5 µM
+ COR 10 µM
+ COR 25 µM

**Figure 7**

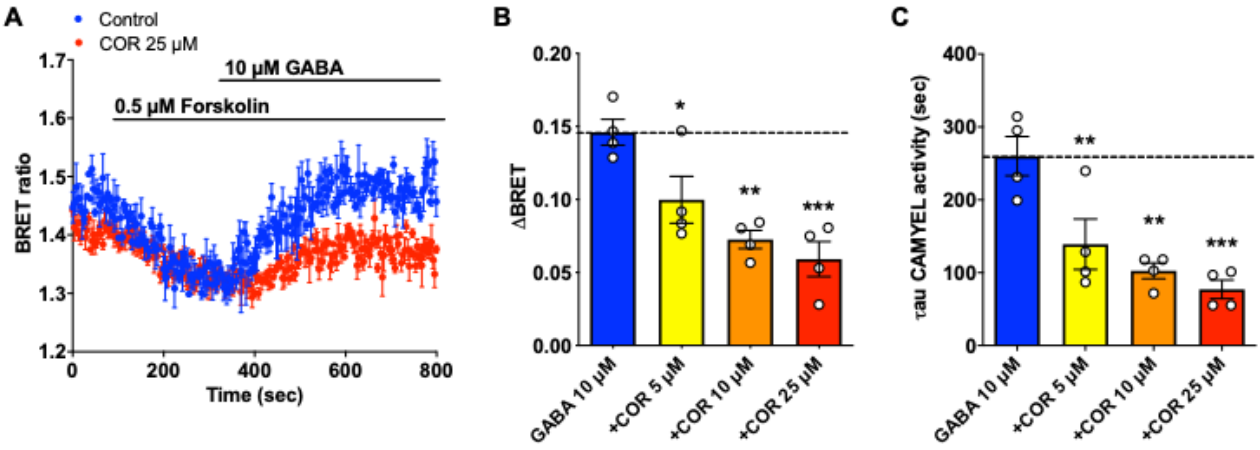
A
Control
COR 25 µM
10 µM GABA
0.5 µM Forskolin
BRET ratio
Time (sec)
B
ΔBRET
GABA 10 µM
+COR 5 µM
+COR 10 µM
+COR 25 µM
C
τau CAMYEL activity (sec)
GABA 10 µM
+COR 5 µM
+COR 10 µM
+COR 25 µM

**Figure 8**

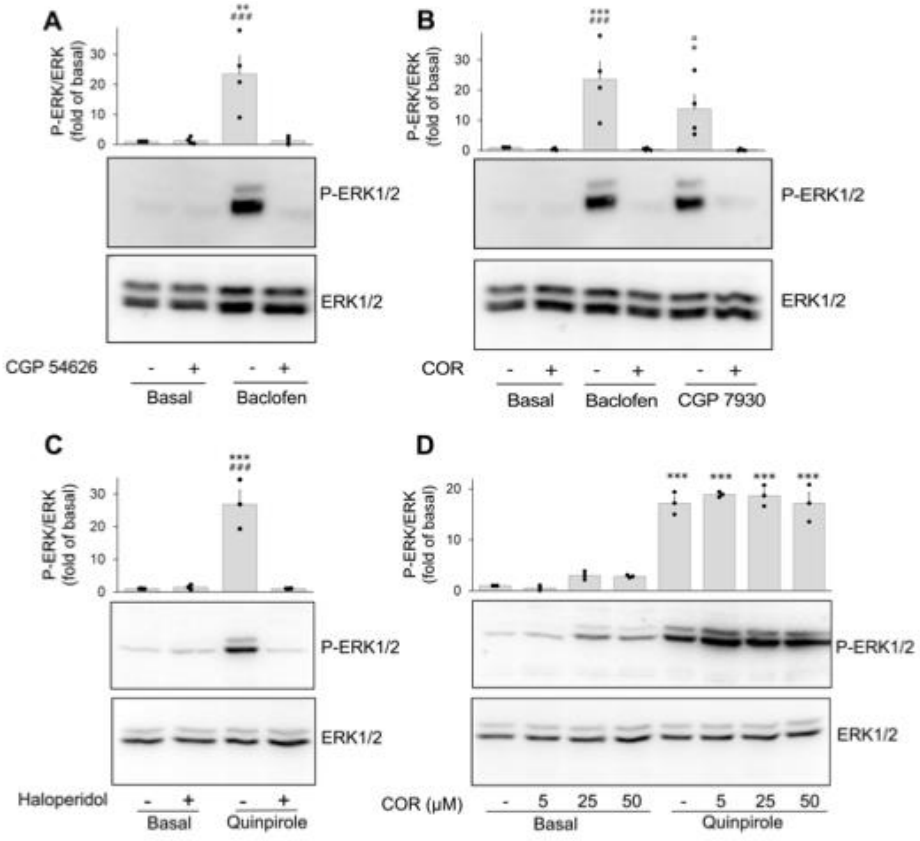
A
B
C
D
P-ERK/ERK (fold of basal)
P-ERK1/2
ERK1/2
CGP 54626
Basal
Baclofen
COR
CGP 7930
Haloperidol
Quinpirole
COR (μM)
5
25
50

**Figure 9**

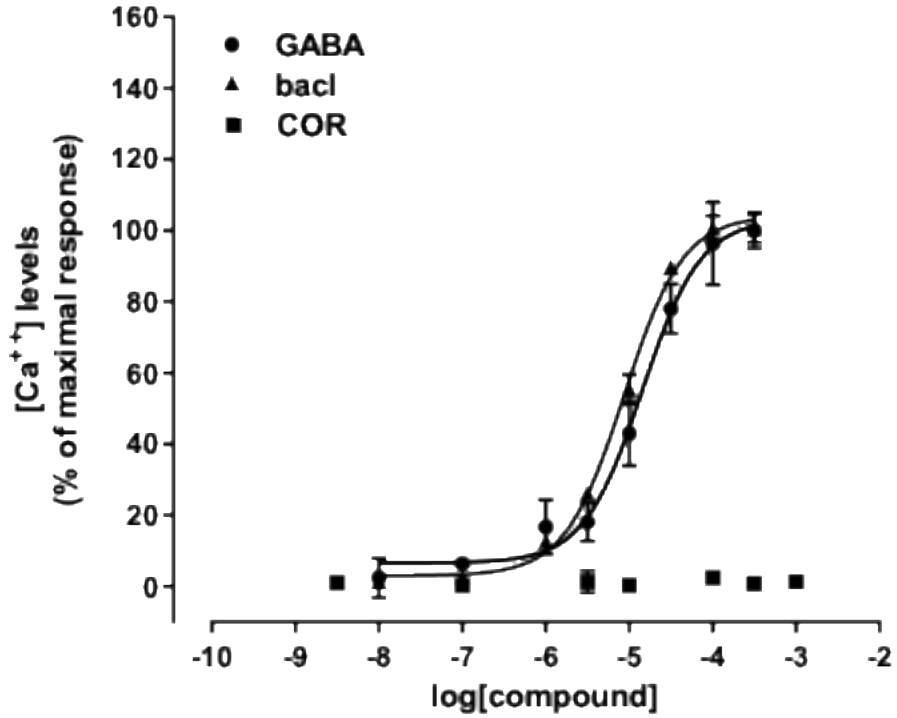
GABA
bacl
COR
[Ca++] levels
(% of maximal response)
160
140
120
100
80
60
40
20
0
-10
-9
-8
-7
-6
-5
-4
-3
-2
log[compound]

**Figure 10**

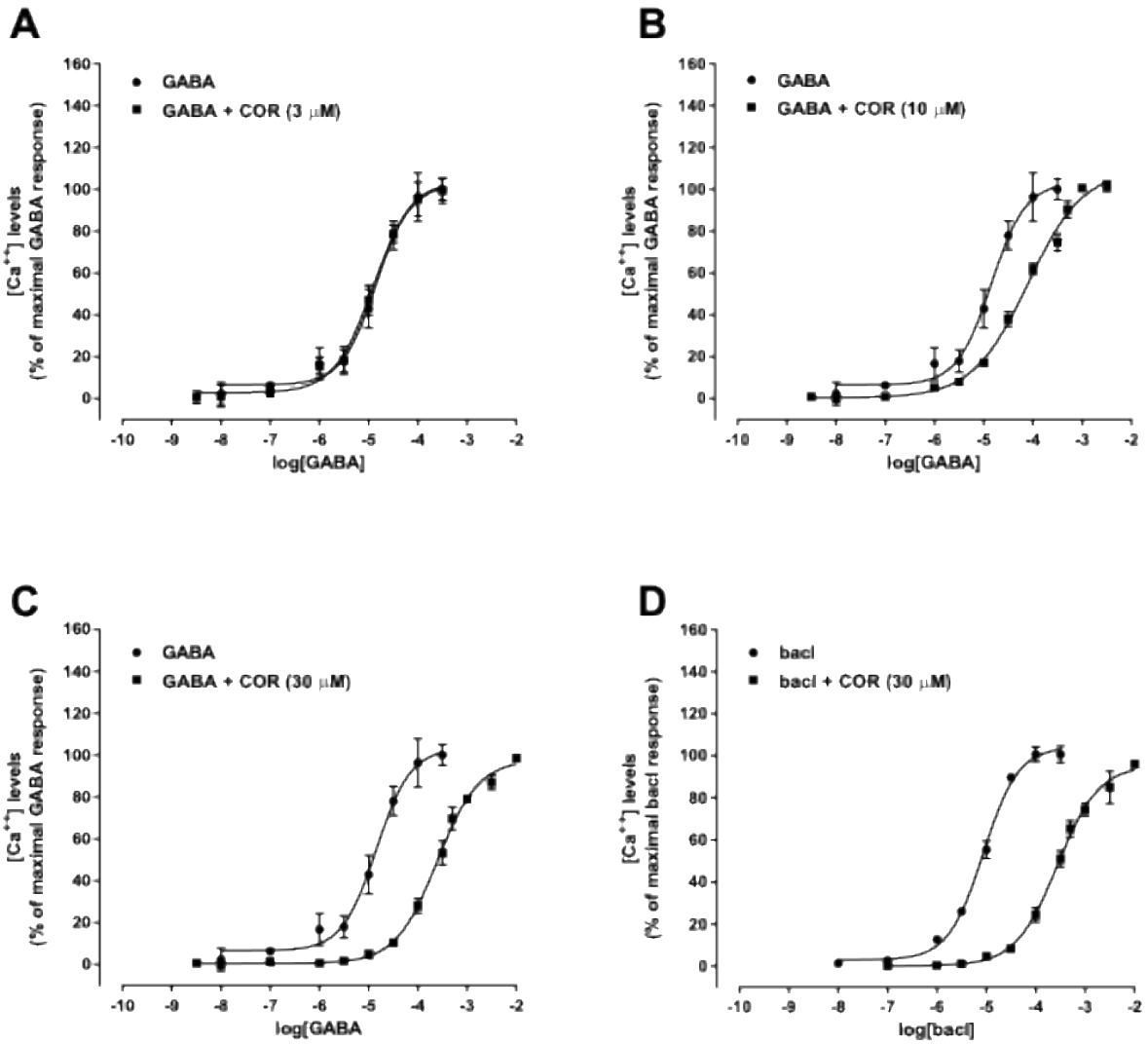
A
GABA
GABA + COR (3 μM)
[Ca++] levels (% of maximal GABA response)
log[GABA]
B
GABA
GABA + COR (10 μM)
[Ca++] levels (% of maximal GABA response)
log[GABA]
C
GABA
GABA + COR (30 μM)
[Ca++] levels (% of maximal GABA response)
log[GABA
D
bacl
bacl + COR (30 μM)
[Ca++] levels (% of maximal bacl response)
log[bacl]

**Figure 11**

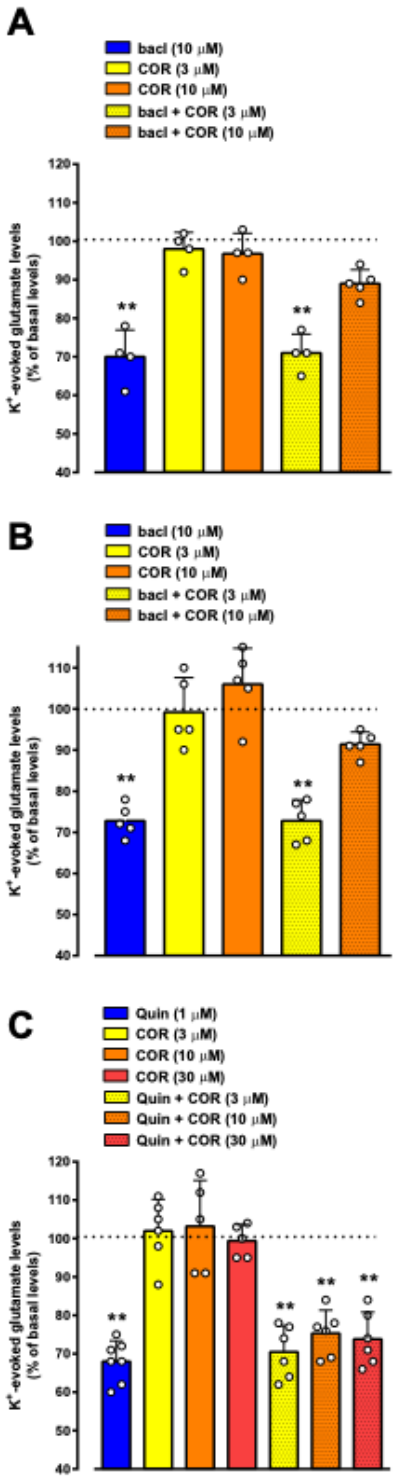


**Figure 12**

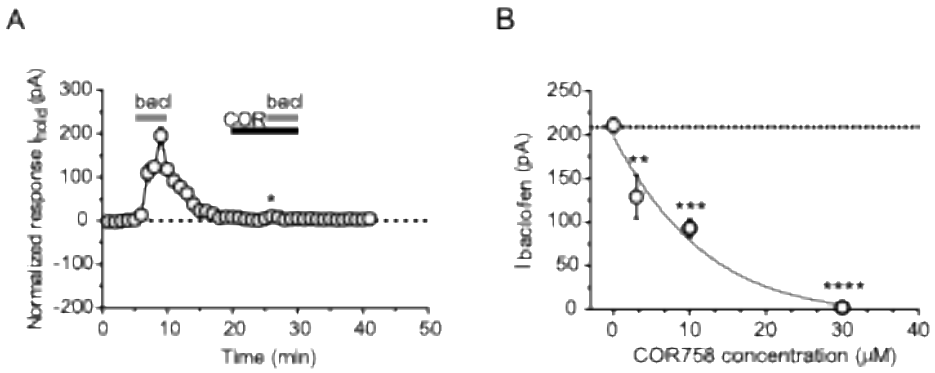
A
B
bacl
COR
bacl
Normalized response Ihold (pA)
Time (min)
Ibaclofen (pA)
COR758 concentration (µM)
**
***
****

**Supplemental Supplemental Figure 1.**

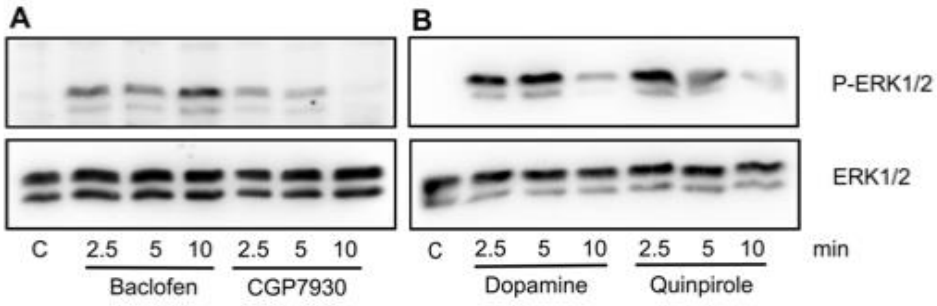

**Supplemental Figure 2.**